THE ASTROPHYSICAL JOURNAL, 162:841–870, December 1970

MAIN-SEQUENCE PHOTOMETRY, COLOR-MAGNITUDE DIAGRAMS, AND AGES FOR THE GLOBULAR CLUSTERS M3, M13, M15, AND M92

ALLAN SANDAGE
Hale Observatories, Carnegie Institution of Washington, California Institute of Technology
Received 1970 July 20

ABSTRACT

New photoelectric photometry is reported for four globular clusters. Distance moduli were found by using nearby field subdwarfs with trigonometric parallaxes for calibration, with account taken of the ultraviolet excess. If one excludes M13, whose RR Lyrae stars may be related to the asymptotic branch rather than the horizontal branch, the RR Lyrae stars in M3, M15, and M92 have $\langle M_V \rangle \simeq +0.6 \pm 0.2$ by this method. The mean is close to values obtained by Woolley *et al.* and van Herk from statistical parallaxes, and by Christy from pulsation theory.

Christy's calculations of absolute magnitudes are consistent with the Oosterhoff-Sawyer effect, and are adopted as a more precise method to obtain luminosities at the termination of the main sequence. Final adopted moduli are $(m - M)_{0,M3} = 14.83$, $(m - M)_{AV,M13} = 14.42$, $(m - M)_{0,M15} = 14.93$, and $(m - M)_{AV,M92} = 14.63$, where the subscripts zero and AV mean true and apparent visual moduli, respectively.

The adopted turnoff luminosities and the helium and metal abundances used for age dating are listed in a table. Ages calculated from Iben and Rood's models average 11.5×10^9 years and have a very small spread. Ages from models by Demarque *et al.* are about 20 percent smaller. These ages show no major conflict with limits for the Friedmann time of the expanding Universe when the present uncertainties in the Hubble constant and the deceleration parameter are considered.

The well-known correlation of the Oosterhoff-Sawyer period-groups with metal abundance is shown to be a natural consequence of the prediction of Simoda and Iben that for clusters of equal age, those with lower metal abundance have brighter luminosities at main-sequence turnoff. The observations and theory are combined to show that the most probable age spread among the four clusters is $\Delta T/T \simeq 0.014$ or $\Delta T \simeq 1.5 \times 10^8$ years as required in the rapid-collapse picture of the Galaxy discussed by Eggen, Lynden-Bell, and Sandage. But the limiting error of the result is high, and permits limits of about $\Delta T \simeq 10^9$ years for the age spread.

Representative points of the C-M diagrams for the four clusters are tabulated in the Appendix.

I. INTRODUCTION

It has been recognized for some time that the ages of globular clusters may closely define the age of the galactic system itself, and possibly set time limits for the Friedmann singularity of the expanding Universe. To make age-dating calculations, it is necessary to have (1) data on the apparent luminosities of main-sequence termination points in clusters of different chemical compositions, (2) the distance to each cluster so apparent magnitudes can be changed to absolute luminosities, (3) the helium and metal abundances of cluster stars, and (4) theoretical evolutionary tracks for stars near the main sequence with a wide range of Y and Z.

It has been nearly 20 years since the main sequences of M92 (Arp, Baum, and Sandage 1953) and M3 (Sandage 1953) were found, and then only with limited accuracy because the photoelectric scale stopped at $V \simeq 19$ and had to be extrapolated into the main-sequence region. In later photometry of M3 (Johnson and Sandage 1956), M13 (Baum *et al.* 1959), and M5 (Arp 1962), adequately faint stars were directly measured for the main-sequence calibration. This material, together with less complete data for ω Cen (Belserene 1959), M2 (Arp 1959), NGC 6397 (Eggen 1960), and 47 Tuc (Tifft 1963) constitute all we presently know about main sequences in globular clusters.

A new observational program on M3, M13, M15, and M92 was started in 1958 to increase the sample. Although the emphasis was on photoelectric observations of very faint stars, special measurements were made of brighter stars to determine the reddening

and helium abundances (Sandage 1969*a*). The complete photometric data for each cluster are given in § II, analysis of the ultraviolet excess in § III, distance determinations in § IV, and an age determination made by using recent theoretical models in § VI.

II. PHOTOMETRIC DATA

a) M3

Photoelectric calibration of M3 was made on the *UBV* system in 1956 (Johnson and Sandage 1956). Measurements of a number of bright stars, and a sequence of twelve faint stars (Table 1 of Johnson and Sandage 1956) in the range $17.7 < V < 21.9$, provided the standards.

In the present program, new photometry was obtained with the Hale 200-inch for many additional faint stars in M3 during five observing seasons between 1960 and 1967. The present pulse-counting system was not then in use at Palomar, and most measurements were made with a d.c. amplifier and strip-chart recorder. The method can give errors as low as 0.02 mag at $V \simeq 21$ if the sample times are adequately long and if the output tapes are carefully integrated.

Table 1 lists the available photoelectric measurements for M3 stars judged to be cluster members from their ultraviolet excess and nearness to the principal sequences, and for probable field stars. For completeness, the brighter stars measured by Johnson (Johnson and Sandage 1956), designated by J in columns (6) and (12), and the horizontal-branch stars previously published (Sandage 1969*a*) are also given.

Formal probable errors were computed for all stars fainter than $V \simeq 18$, based on the scatter in the individual star-plus-sky, minus sky deflections. As many as forty such differences were obtained for each of the fainter stars, each deflection lasting about 30 seconds on and off the source. The probable errors average ± 0.03 mag in all three colors; the largest errors are for star F25 where $\epsilon(V) = \pm 0.091$, $\epsilon(B) = \pm 0.031$ mag.

But much more serious than the random statistics are systematic errors due to background and crowding effects, which can often reach values larger than 0.1 mag. To test for such systematic effects, four 200-inch plates in each color (103a-O + GG13 for B, and 103a-D + GG11 for V) were measured to smooth the faint sequence. Results in Table 2 should provide the best currently available values for the position of the M3 main sequence. Also listed are $U - B$ values obtained by using the smoothed B_{pg} magnitude and the photoelectric U_{pe} value from Table 1. This is only a partial smoothing of $U - B$, but is the best that can be done from the present material since no photographs were taken in U.

All stars listed in Tables 1 and 2 are identified on one or more of the three finding charts of M3 shown in Figures 1, 2, and 3 (Plates 5, 6, 7), as indicated in columns (2) and (8) of Table 1.

The C-M diagram from stars in Table 1 is shown in Figure 4. The five crosses are stars believed to be blue stragglers in M3. Photoelectric measurement of these stars was exceedingly difficult due to crowding and background problems, but the five plotted and listed in Table 1 with asterisks are believed to have moderately reliable photometry. Each star shows an ultraviolet excess (§ III) that is consistent with cluster membership.

b) M13

Photometry of the bright stars in M13 is available from data published by Baum (1954), Arp (1955), Brown (1955), Arp and Johnson (1955), Savedoff (1956), and Kadla (1968). The main sequence was first isolated in 1954 by Baum, but new data obtained in 1959 for twenty-four stars fainter than $V = 19$ (Baum *et al.* 1959) showed that this early-main-sequence position was too blue by $\Delta(B - V) \simeq 0.15$ mag for stars fainter than $V \simeq 18$. The effect was to place the 1954 sequence too faint by $\Delta V \simeq 0.8$ mag at a given color.

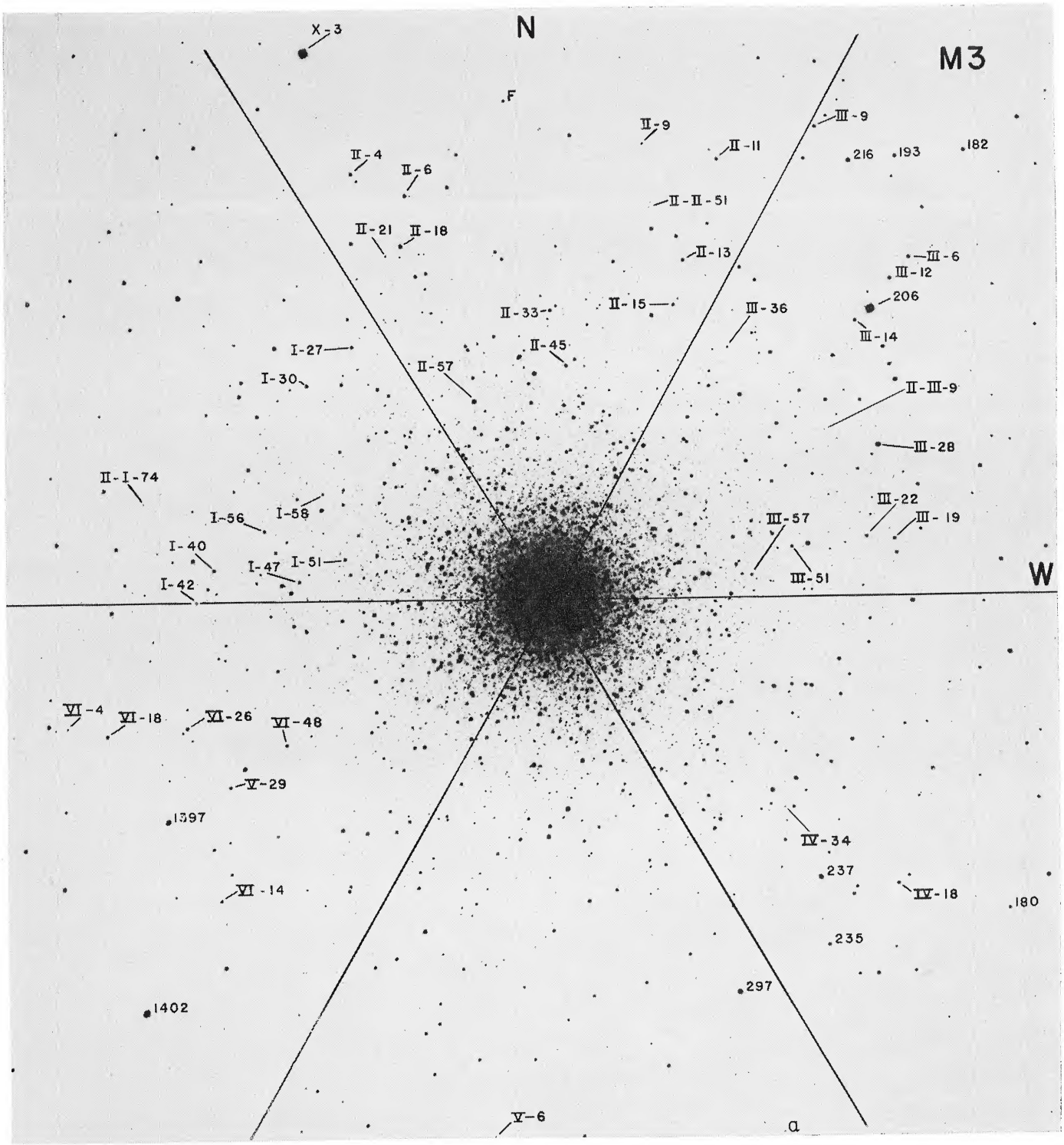

FIG. 1.—Finding chart for the brighter stars in M3 that are listed in Table 1. Photograph is an unfiltered blue plate taken with the Mount Wilson 100-inch Hooker reflector. Called M3 Chart 1 in the tables.

SANDAGE (*see* page 842)

PLATE 6

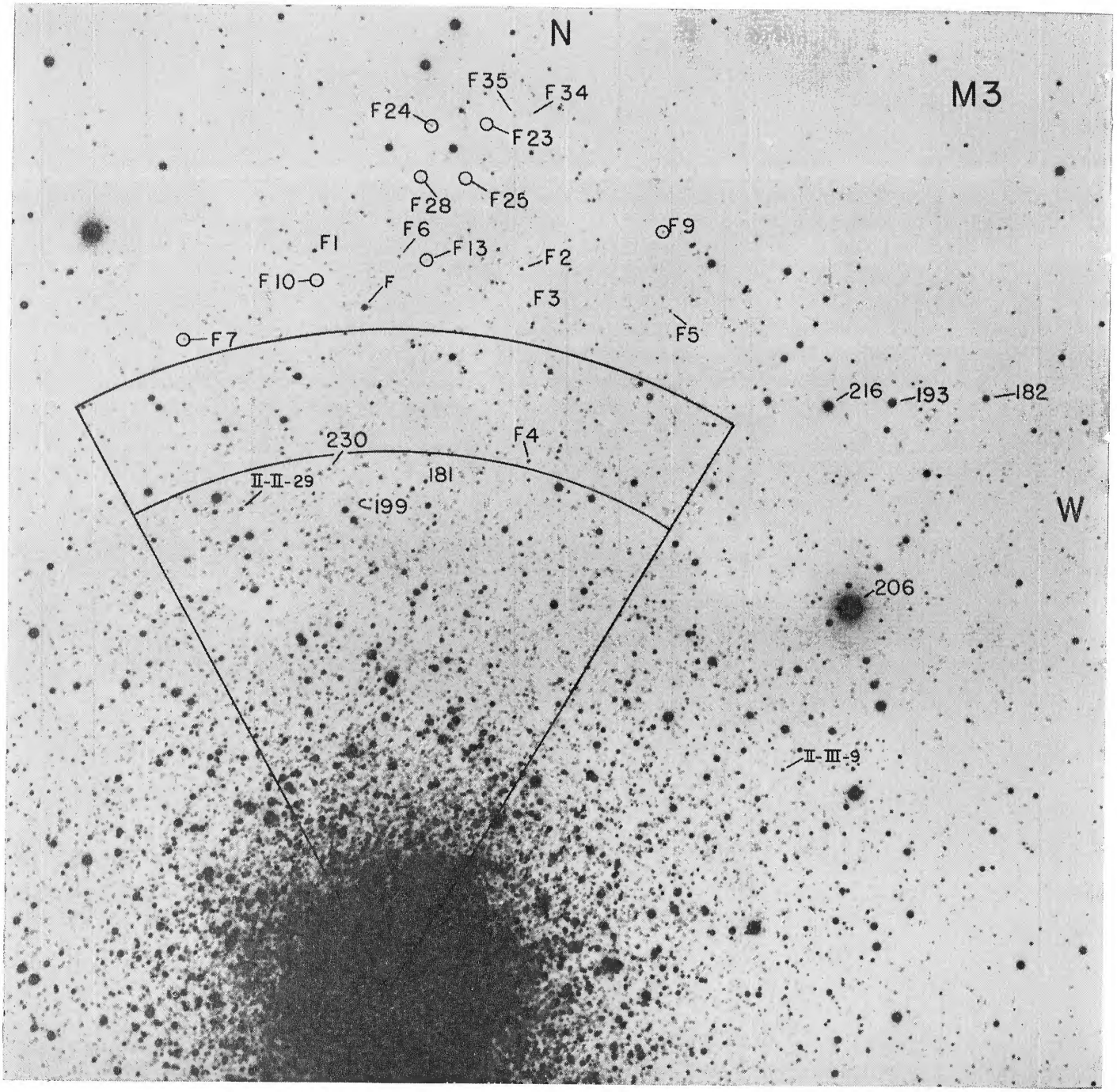

FIG. 2.—Chart for faint stars in M3 listed in Table 1. Blue plate taken with the 200-inch Palomar Hale reflector on 103a-O + GG13. Called M3 Chart 2 in the tables.

SANDAGE (*see* page 842)

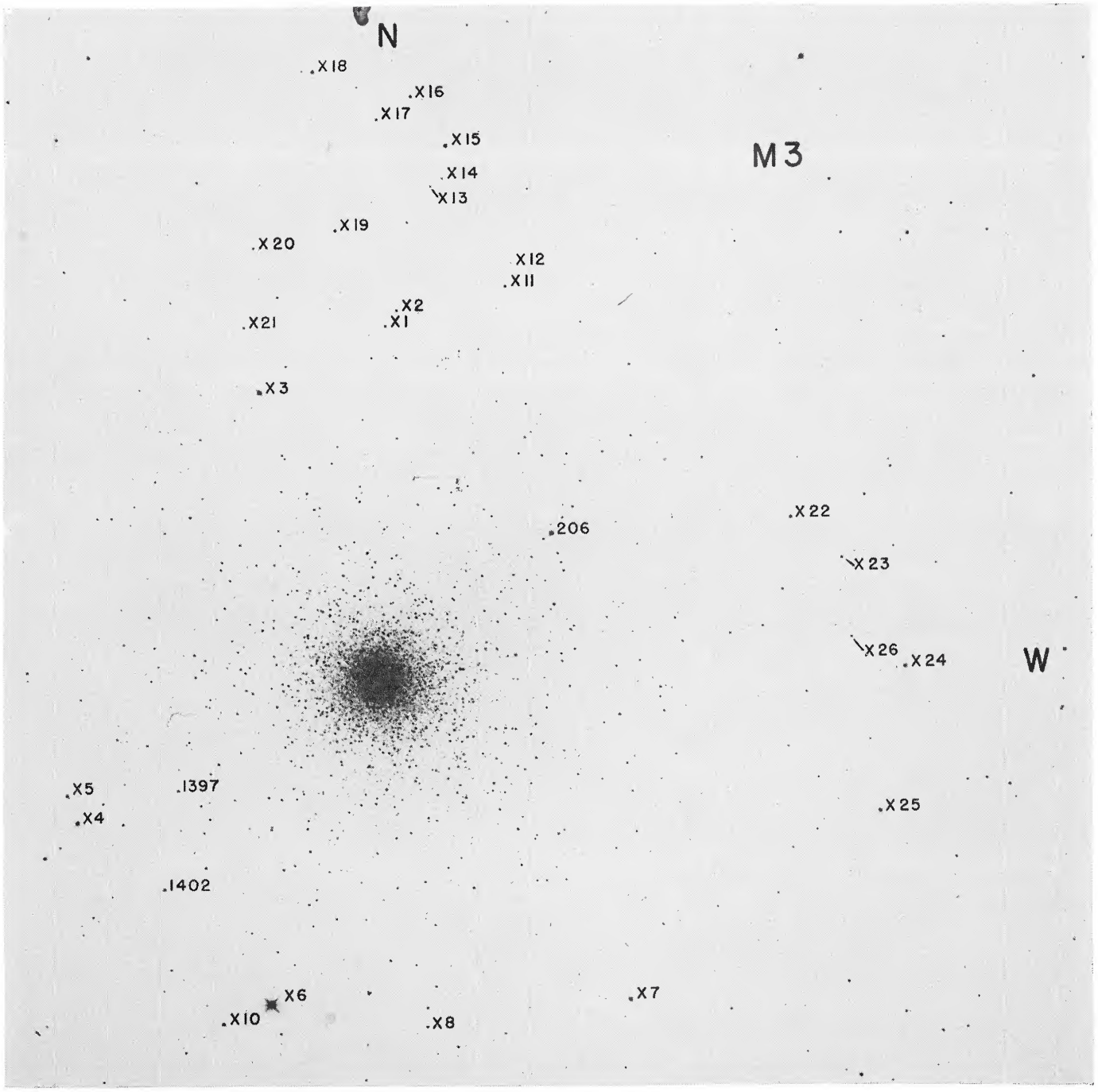

FIG. 3.—Wide field around M3 taken with the Mount Wilson 60-inch diaphragmed to 40 inches on unfiltered 103a-O. Called M3 Chart 3 in the tables. Photoelectric values are listed in Table 1, Part 2.

SANDAGE (*see* page 842)

TABLE 1

PHOTOELECTRIC DATA FOR STARS IN AND NEAR M3

Star	Chart	V	B-V	U-B	n	Star	Chart	V	B-V	U-B	n
PROBABLE MEMBERS											
1397	1,3	12.65	+1.56	+1.63	J(82)	I-II-4	1	15.86	+0.08	-0.03	1(J)
I-III-28	1	12.81	+1.37	+1.26	J(82)	I-VI-48	1	15.90	+0.02	+0.06	1(200)
297	1	12.89	+1.42	+1.40	1(200),J	I-I-27	1	16.14	-0.02	+0.01	2(200)
X-23	3	13.26	+1.29	+1.16	1(100)	I-I-56	1	16.28	-0.07	-0.16	1(200)
X-2	3	13.84	+0.95	+0.56	1(60)	I-I-47	1	16.37	-0.10	-0.22	1(200)
216	1,2	14.09	+1.01	+0.62	2(200),J	I-II-9	1	16.74	+0.71	+0.05	1(J)
I-II-18	1	14.09	+0.94	+0.49	J(82)	a	1	16.86	+0.75	-0.01	1(J)
193	1,2	14.80	+0.89	+0.36	6(200),J	I-III-57†	1	16.95:	-0.21:	-0.47:	1(200)
I-II-57	1	14.94	-0.30	-1.11	2(200),J	I-VI-4	1	17.00	+0.71	+0.07	1(200)
I-III-19	1	15.46	+0.42	+0.00	1(200)	I-I-58†	1	17.10:	-0.12:	-0.55:	1(200)
I-III-51	1	15.46	+0.50	-0.01	1(200)	I-V-6*	1	17.41	+0.21	0.00	1(200)
I-II-33	1	15.57	+0.14	+0.08	1(200)	I-III-36*†	1	17.47:	+0.19:	+0.01:	1(200)
I-I-42	1	15.58	+0.44	+0.02	1(200)	F1	2	17.75	+0.70	-0.04	1(J)
I-II-15	1	15.61	+0.45	-0.03	1(200)	III-II-181†	2	18.12	+0.60	-0.11	1(200)
I-III-9	1	15.61	+0.48	-0.01	5(200)	F2	2	18.38	+0.60	-0.12	1(J)
I-II-6	1	15.61	+0.08	+0.14	1(J)	II-I-74*†	1	18.45	+0.20	-0.10	1(200)
I-III-22	1	15.62	+0.12	+0.05	1(200)	II-II-51*	1	18.46	+0.33	-0.14	1(200)
I-II-45	1	15.64	+0.12	+0.10	1(200)	II-III-9*†	1	18.46	+0.31	-0.10	1(200)
I-I-40	1	15.68	+0.39	0.00	1(200)	III-II-230†	2	18.50	+0.52	-0.20	1(200)
I-II-11	1	15.68	+0.42	-0.03	1(J)	F5	2	18.94	+0.35	-0.20	2(200)
I-VI-29	1	15.68	+0.42	+0.03	1(200)	F6	2	19 06	+0.43	-0.16	2(200)
182	1,2	15.70	+0.08	+0.11	25(200)	III-II-199†	2	19.11	+0.40	.....	1(200)
I-VI-18	1	15.70	+0.16	+0.05	1(J)	F7	2	19.71	+0.40	-0.12	1(200)
I-III-6	1	15.71	+0.08	+0.09	1(200)	F24	2	19.75	+0.39	-0.17	3(200)
I-III-12	1	15.71	+0.08	+0.10	1(200)	F35	2	19.87	+0.48	-0.06	1(200)
I-IV-18	1	15.73	+0.12	+0.05	1(200)	F34	2	20.00	+0.45	-0.17	1(200)
"	1	15.95	-0.01	-0.02	1(J)	F9	2	20.41	+0.54	.....	1(200)
I-II-13	1	15.76	+0.09	+0.16	1(200)	F10	2	20.46	+0.52	-0.02	1(200)
I-III-14	1	15.76	+0.09	+0.11	1(200)	F13	2	20.49	+0.31	-0.16	2(200)
I-VI-26	1	15.76	+0.01	+0.05	1(200)	F28	2	20.68	+0.62	-0.02	1(200)
235	1	15.76	+0.08	+0.13	1(200)	F23	2	21.04	+0.64	.....	2(200)
I-I-30	1	15.82	+0.01	+0.01	2(200)	F25	2	21.12	+0.47	.....	2(200)
I-I-51	1	15.82	+0.07	+0.13	1(200)						
PROBABLE FIELD											
X6	3	8.42	0.42	-0.02	1(60)	X1	3	13.97	0.63	0.01	1(60)
206	1,2,3	9.85	1.15	1.06	7(100),40(200)	237	1	14.09	0.65	0.10	J(82)
X3	1,3	10.54	0.66	0.17	1(6),1(1),1(2)	X16	3	14.18	0.56	0.00	1(100)
X7	3	11.46	0.69	0.10	1(60)	X17	3	14.28	0.62	0.08	1(100)
X4	3	11.74	0.64	0.16	1(60)	X20	3	14.71	0.92	0.69	1(100)
X-25	3	11.86	0.80	0.36	1(100)	X26	3	15.09	0.92	0.62	1(100)
X-15	3	11.87	0.60	0.04	1(100)	X14	3	15.22	1.02	0.98	1(100)
X-18	3	12.63	0.75	0.28	1(100)	180	1	15 23	1.11	1.03	J(82)
X-22	3	12.64	0.64	0.12	2(100)	X13	1	15.42	0.81	0.35	1(100)
1402	1,3	12.66	0.64	0.09	1(6),1(2)	I-VI-14	1	15.68	0.72	0.20	J(82)
X10	3	12.72	0.74	0.29	1(60)	F	2	16.02	0.56	-0.09	2(200)
X24	3	12.78	0.57	-0.04	1(100)	X12	3	16.96	0.32	0.11	1(100)
X5	3	12.91	0.75	0.23	1(60)	I-II-21	1	17.23	0.40	-0.09	1(200)
X19	3	13.51	0.55	-0.05	1(100)	II-II-29†	2	17.59	0.45	-0.01	1(200)
X11	3	13.89	0.47	0.03	1(100)	I-IV-34†	1	17.74	0.13	0.15	1(200)
X8	3	13.95	1.15	0.98	1(100)	F3	2	18.39	0.71	0.20	J(82)
X21	3	13 96	0.67	0.16	1(100)						

* Possible blue stragglers from "probable members" section. Photoelectric photometry very difficult because of crowding problems.

† Possibility of crowding uncertainties in photometry due to closeness to the center.

The present program was carried out between 1960 and 1967 to supplement the 1959 photometry. A number of stars near the main-sequence turnoff were measured, together with horizontal-branch and field stars. Part of the new data have been published elsewhere (Sandage 1969*a*, Table 3), and the remainder are listed in Table 3 here. The stars can be identified either on the chart given in Baum *et al.* (1959, Fig. 1) or in Figure 5 (Plate 8) of this paper as indicated in column (7) of Table 3.

Formal probable errors were calculated from the mean deviations of the on-off deflections. They average 0.015 mag in all colors for stars in Table 3, but again, systematic crowding errors are more important and these can be partially eliminated by photographic smoothing. Four 200-inch photographic plates were measured in each color by

TABLE 2

PHOTOGRAPHIC VALUES FOR PHOTOELECTRIC STARS IN M3 FOR $V > 17$*

Star	V	$B-V$	$U_{pe}-B_{pg}$	Star	V	$B-V$	$U_{pe}-B$*
I-I-58	16.94	(−0.10):	...	F6	19.02	0.41	−0.10
I-II-21†	17.23	0.31	0.00	III-II-199	18.79	0.41	...
I-III-36	17.45	0.26	−0.04:	F7	19.66	0.40	−0.07
II-II-29†	17.80	0.26	−0.03	F24	19.71	0.41	−0.15
F1	17.83	0.68	−0.10	F35	19.90	0.44	−0.05
III-II-181	18.03	0.68	−0.10	F34	20.23	0.47	−0.42:
F2	18.50	0.54	−0.18	F9	20.21	0.56	...
F3†	18.44	0.73	+0.13	F10	20.43	0.49	+0.04
II-II-51	18.45	0.35	−0.15	F13	20.25	0.46	−0.07
II-III-9	18.41	0.31	−0.05	F28	20.71	0.64	−0.07
III-II-230	18.58	0.42	−0.18	F23	21.05	0.65	...
F5	18.94	0.40	−0.25	F25	20.74	0.54	...

* Based on four 103aO + GG13 plates for B (measured once each) and four 103a-D + GG11 plates for V (measured once).
† Probable field star.

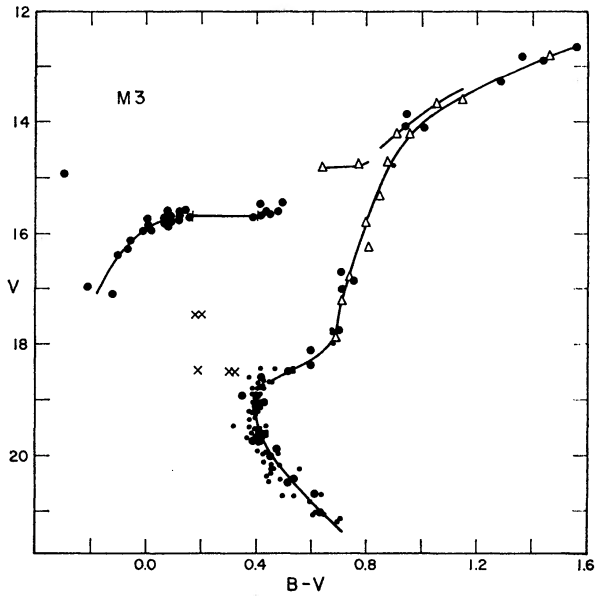

FIG. 4.—C-M diagram for M3 from data in Table 1. *Open triangles*, normal points from a previous photographic study. *Crosses*, possible blue stragglers. *Small dots*, photographic values from an unpublished study of the main sequence by Katem and Sandage. No reddening or absorption corrections have been applied.

PLATE 8

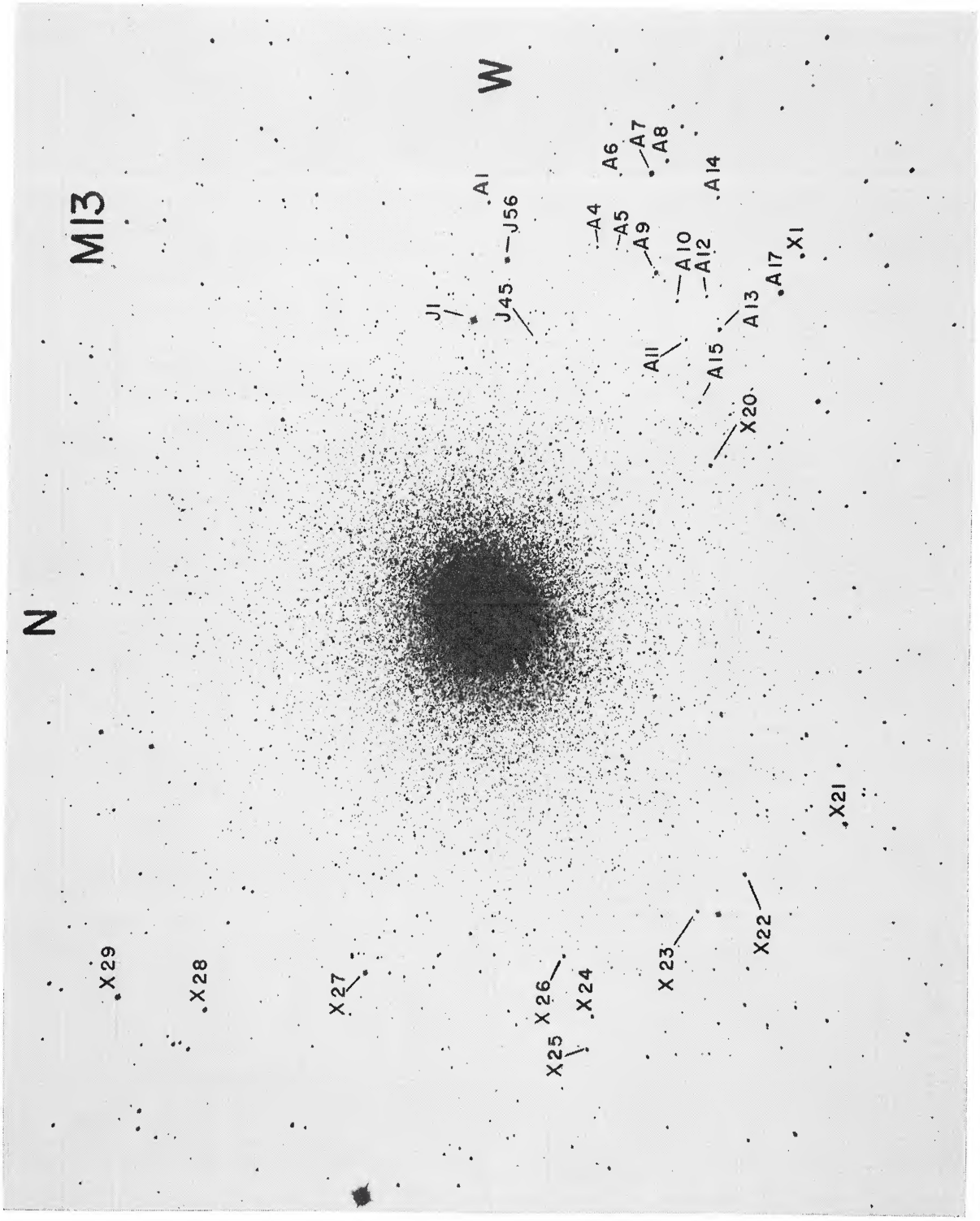

FIG. 5.—Finding chart for M13 for stars listed in Table 3 which are not identified by Baum *et al.* (1959). Photograph is from an unfiltered blue plate taken with the 100-inch reflector.

SANDAGE (*see* page 844)

Katem relative to the entire list of standards now available (Table 3 here and Table 1 of Baum *et al.* 1959). The results are listed in Table 4, and supersede the data given previously (Baum *et al.* 1959, Table 3). Comparison of Tables 3 and 4 of the present paper shows that no color or magnitude equation exists; the data of Table 4 are therefore systematically on the *BV* photoelectric system.

TABLE 3

NEW PHOTOMETRY IN M13

Star (1)	V (2)	$B-V$ (3)	$U-B$ (4)	n 60 (5)	n 200 (6)	Chart* (7)
			Members			
A1	13.39	1.05	+0.68	...	7	3
X24	13.75	0.95	+0.605	2	...	3
A10	14.33	0.88	+0.41	...	7	3
A12	15.59	0.84	+0.31	...	1	3
A4	15.91	0.79	+0.22	...	1	3
B24	17.455	0.76	+0.15	...	2	2
38	17.95	0.50	−0.08	...	1	2
20	17.96	0.49	−0.17	...	1	2
80	18.15	0.45	−0.19	...	1	2
90	18.21	0.45	−0.17	...	1	2
69	18.24	0.40	−0.20	...	2	2
183	18.56	0.44	−0.21	...	1	2
178	18.56	0.41	...	...	1	2
66	18.59	0.45	−0.21	...	1	2
17	18.62	0.49	...	...	1	2
150	18.64	0.42	...	...	1	2
H	18.72	0.45	−0.10	...	1	2
B28	18.83	0.43	−0.12	...	1	2
			Field Stars			
A17	10.66	1.39	+1.65	...	1	3
J1	10.74	0.58	+0.066	...	14	1,3
J56	10.886	1.117	+1.10	...	11	1,3
A7	11.07	1.21	+1.21	...	1	3
X27	11.30	0.93	+0.54	1	...	3
X1	11.51	1.50	+1.21	...	1	3
X20	11.80	1.28	+1.24	2	...	3
X29	11.88	0.40	−0.05	1	...	3
X28	12.35	0.70	+0.10	1	...	3
X21	12.36	0.48	−0.07	2	...	3
A13	12.36	1.04	+0.88	...	2	3
A9	12.44	0.66	+0.18	...	1	3
X22	12.60	0.85	+0.51	2	...	3
X23	13.16	1.38	+1.52	2	...	3
X26	13.49	0.71	+0.27	1	...	3
X25	13.56	0.86	+0.50	2	...	3
A8	13.74	0.67	+0.11	...	1	3
A15	14.22	0.58	+0.06	...	1	3
A14	14.70	0.68	+0.20	...	1	3
J45	14.98	0.76	+0.30	A, J	...	1,3
A6	16.33	0.60	+0.02	...	1	3
A5	16.45	1.50	...	...	1	3

* Chart references:
1. Arp and Johnson (1955), Fig. 4.
2. Baum *et al.* (1959), Fig. 1.
3. This paper.

The C-M diagram for M13 is shown in Figure 6. Only photoelectric data are plotted as taken from the following sources. Brighter than $V \simeq 17$ part of the data are from Baum (1954) as transformed from his $P_0 - V$ system to $B - V$ by $B - V = 0.917\ (P_0 - V) + 0.16$ as given in his paper. Data directly on the $B - V$ system are taken from Arp and Johnson (1955, Table 1), and from Sandage (1969*a*, Table 3). Fainter than $V = 17$, the new data from Table 3, as smoothed in Table 4, are plotted. Open triangles are mean photographic points read from Figure 1 of Arp and Johnson (1955). No reddening corrections have been applied. Two RR Lyrae stars studied by Arp (1955) are plotted at their transformed magnitudes of $V = 14.55$, $B - V = 0.42$ for Sawyer No. 7, and $V = 14.59$, $B - V = 0.46$ for Sawyer No. 8. The peculiar position of these variables is discussed in § V.

TABLE 4

M13 PHOTOGRAPHIC VALUES OF PROBABLE-ERROR STANDARDS; MEAN OF FOUR PLATES IN EACH COLOR

Star	V_{pg}	$(B-V)_{pg}$	$U_{pe}-B_{pg}$	Star	V_{pg}	$(B-V)_{pg}$	$U_{pe}-B_{pg}$
J55	16.92	0.65	−0.01	I	19.85	0.51	−0.08
J51	17.15	0.66	+0.16	E	19.80	0.62	+0.35?
B24	17.47	0.75	+0.15	77	20.01	0.50	...
38	17.96	0.52	−0.09	108	20.16	0.53	−0.16
20	17.94	0.46	−0.14	F	20.40	0.69	−0.22
80	18.14	0.44	−0.18	G	20.43	0.60	−0.16
90	18.24	0.44	−0.18	Z	20.66	0.63	...
69	18.26	0.42	−0.24	W	20.55	0.61	...
183	18.48	0.43	−0.12	23	20.49	0.54	...
178	18.55	0.49	...	D	20.57	0.68	...
66	18.62	0.48	−0.17	N	21.19	0.88	...
17	18.56	0.46	...	B	20.92	0.70	...
150	18.57	0.51	...	T	20.99	0.85	...
H	18.69	0.40	−0.02	S	21.20	0.65	...
B28	18.83	0.44	−0.13	M	21.23	0.83	...
L	19.15	0.46	−0.22	Y	21.42	0.88	...
P	19.53	0.52	−0.15	O	21.52	0.82	...
K	19.51	0.51	−0.08	U	21.50	0.95	...
36	19.44	0.49	−0.18	R	21.30	0.78	...

c) M15

Photometry of M15 on the old International System to $V \simeq 17$ has been published by Brown (1951) and Arp (1955). In the present program, *UBV* measurements were made for two purposes. (1) An initial standard sequence reaching $V \simeq 17$ was established between 1958 and 1960 with the 100-inch reflector to calibrate *UBV* plates taken for the RR Lyrae stars (Sandage *et al.* 1971). (2) In the 1961–1967 seasons, the calibration was extended to $V = 22$ with the Hale 200-inch telescope to locate the main sequence. All the data obtained in these programs are given in Tables 5–8.

Table 5 lists data for cluster members in the range $13 < V < 22$. The first section gives photoelectric values, measured on the number of nights and with the telescopes listed in columns (7) and (8). Probable errors for stars fainter than $V \simeq 18$ are all less than 0.08 mag, and average ~0.03 mag in each color.

As by-products of other programs, the photoelectric data have been extensively smoothed by using photographic plates, with the results listed in the second section of Table 5. Stars used for standards in the unpublished RR Lyrae photometry were measured on sixty-three plates in *V*, sixty-one plates in *B*, and thirty-nine plates in *U*, as

shown in the final column. Stars measured in the special program for gaps in the giant branch (Sandage, Katem, and Kristian 1968) were measured on ten plates in B and V; faint main-sequence stars were smoothed by Katem on five plates in each color, measured once brighter than $V = 19$, and measured twice fainter than this limit.

During the study of the bright part of the luminosity function, where every uncrowded star brighter than $V = 17$ was measured photographically (Sandage *et al.* 1968), many stars were located at the blue end of the horizontal branch. Most of these are so close to the center of the cluster that photoelectric photometry was impossible. Those that could be measured are listed in parentheses in Table 5. The photometry is moderately reliable for them, but is not as precise as for other stars in the table.

Table 6 gives photoelectric data for probable field stars. The column marked n shows the number of observations with various telescopes: S and H stand for the Mount Wilson 60- and 100-inch, and P for the Palomar Hale 200-inch.

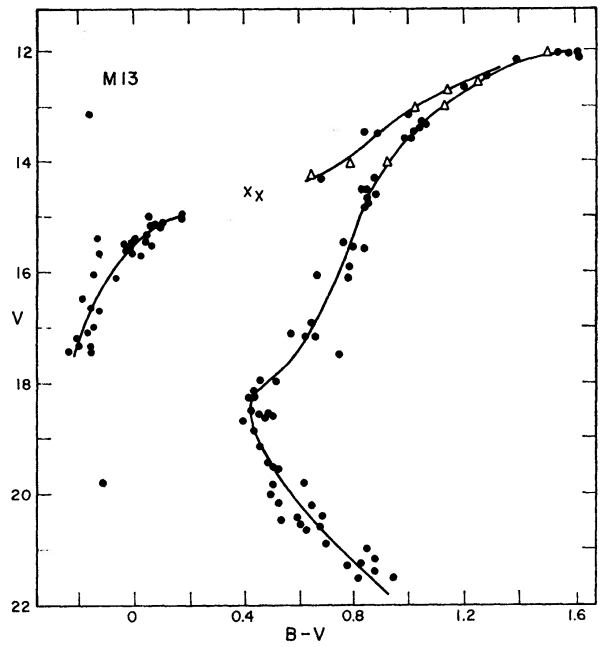

FIG. 6.—C-M diagram for M13 from data listed in the text. No reddening or absorption corrections have been applied.

Table 7 lists additional main-sequence stars which were originally chosen for photoelectric measurement but which were not so observed. The listed values have high weight because of repeated photographic measurement on the same system as Table 5. They are kept to help define the position of the main-sequence knee.

Stars in Table 8 were used as secondary standards for the RR Lyrae program already mentioned. The listed values depend on measurements of sixty-three plates in V, sixty-one in B, and thirty-nine in U. The column marked *branch* shows to which sequence the star belongs. The notation is the same as for M92 (Sandage and Walker 1966) where A is the giant branch, B are subgiants, C the asymptotic branch, D the horizontal branch, and F are supposed field stars.

The stars in Tables 5–8 are identified on the four charts of M15 shown in Figures 7–10 (Plates 9–12). The columns marked *chart* in the tables indicate on which map the star is to be found.

The C-M diagram derived from the complete photoelectric data is shown in Figure 11.

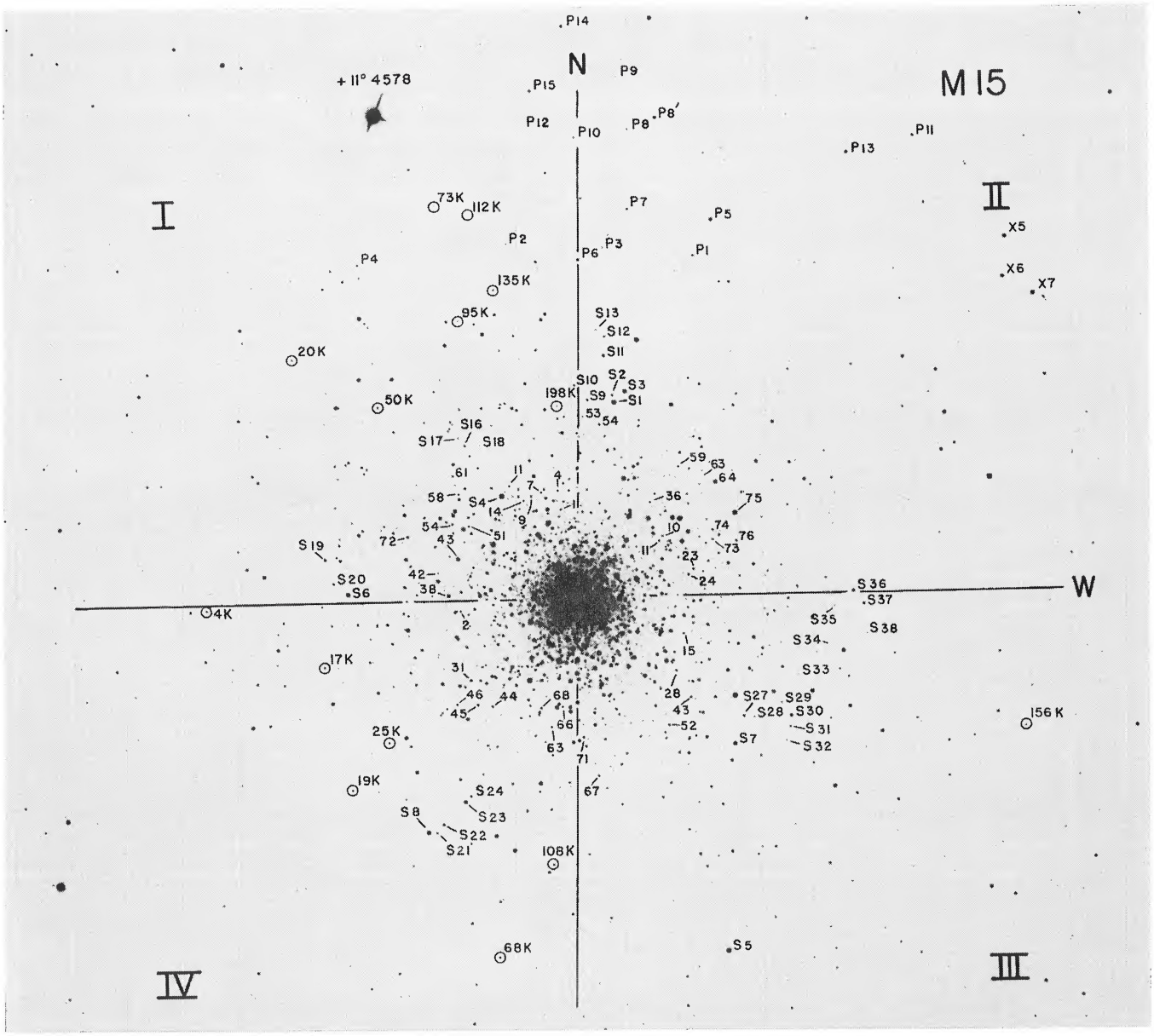

FIG. 7.—Finding chart for the bright standards in M15 used for the RR Lyrae photometry, plus special fainter stars. Yellow plate taken with the 100-inch diaphragmed to 58 inches on 103a-D + GG11. Called M15 Chart 1 in Tables 5, 6, and 8.

SANDAGE (*see* page 847)

PLATE 10

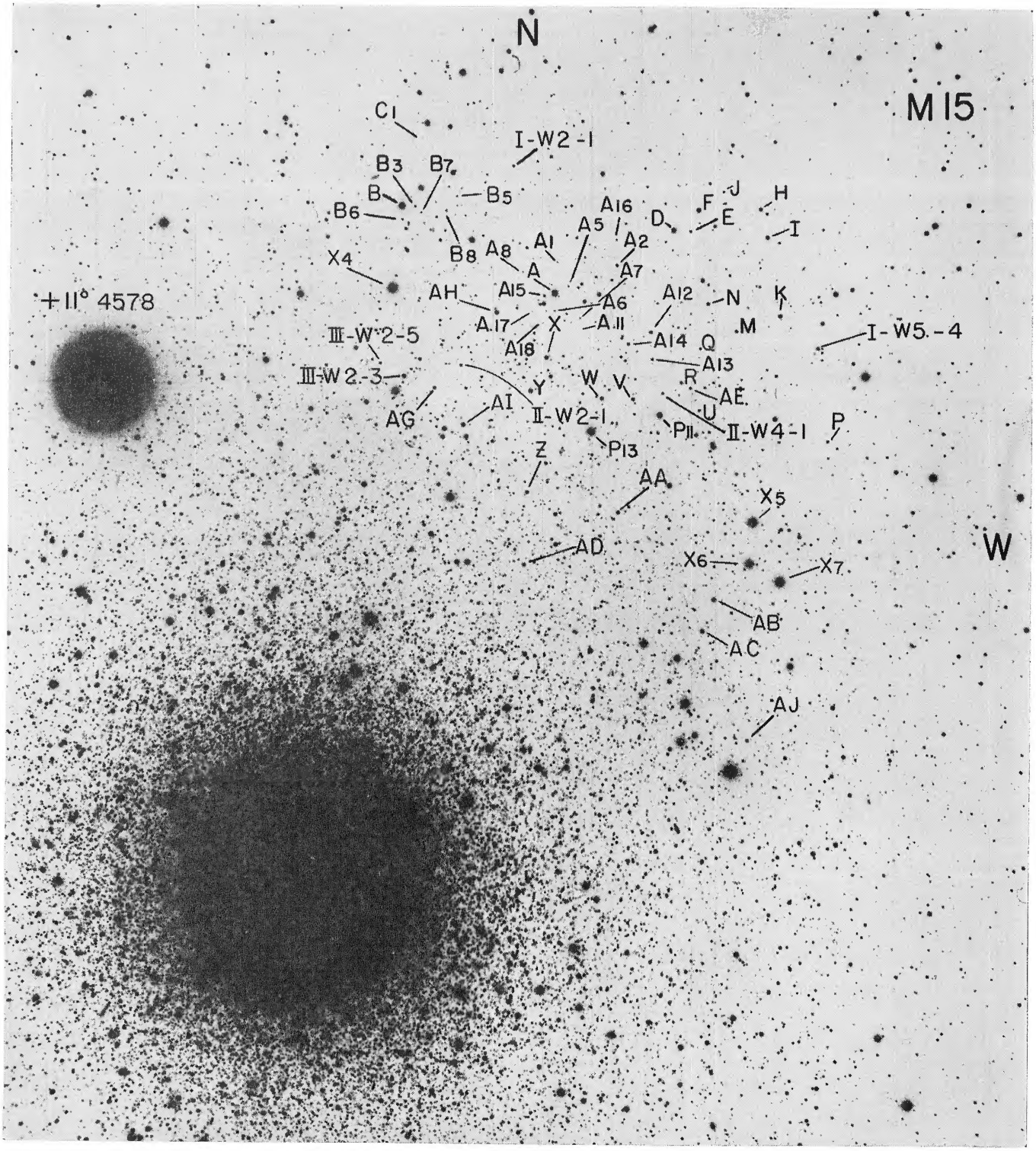

FIG. 8.—Finding chart for the faint stars in M15 that are listed in Tables 5 and 6. Yellow plate taken with the 200-inch reflector on 103a-D + GG11. Called M15 Chart 2 in the tables.

SANDAGE (*see* page 847)

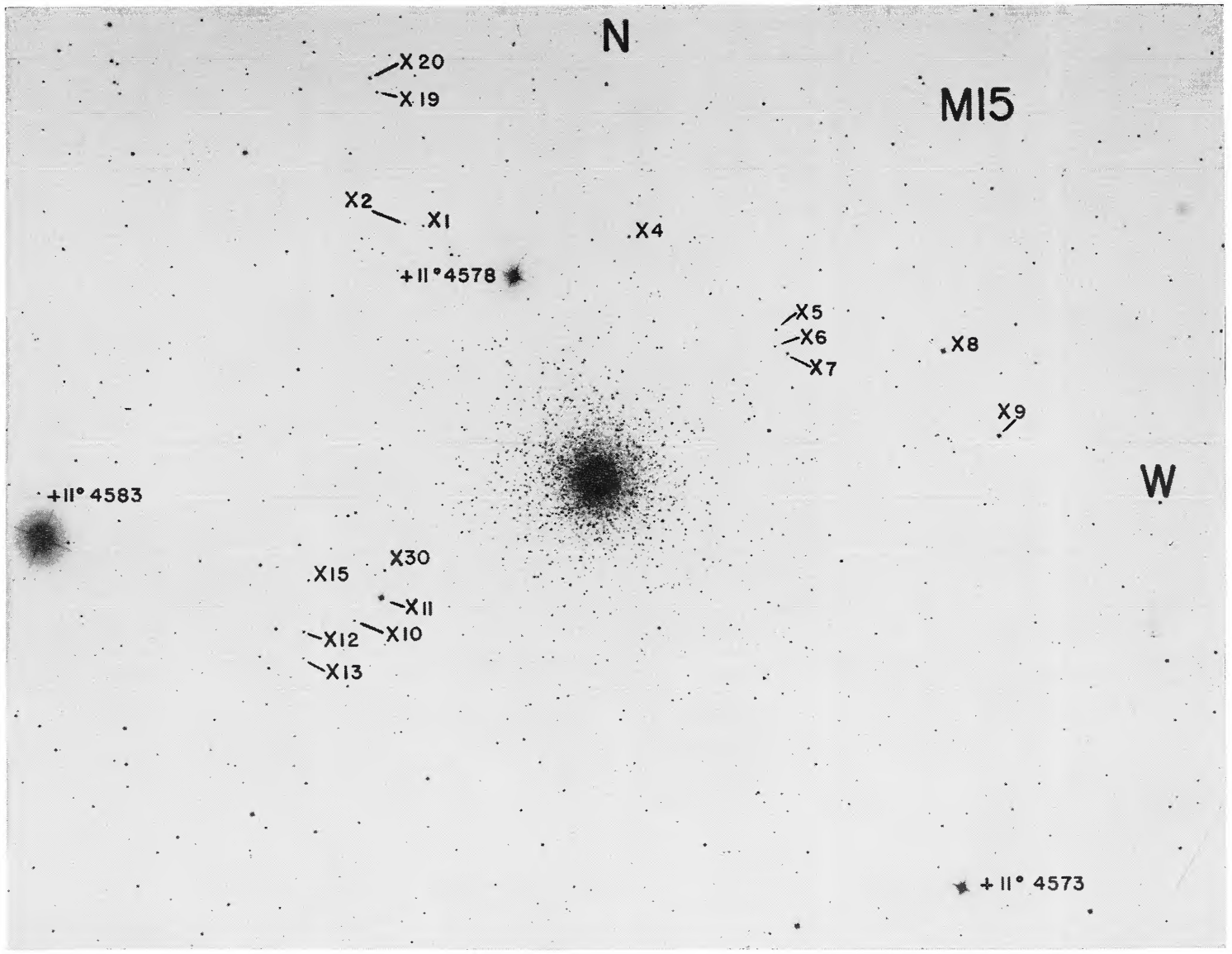

FIG. 9.—Wide field around M15 taken with the 100-inch diaphragmed to 58 inches on IIa-O + GG13. Photometric values are listed in Tables 5 and 6. Called M15 Chart 3 in the tables.

SANDAGE (*see* page 847)

PLATE 12

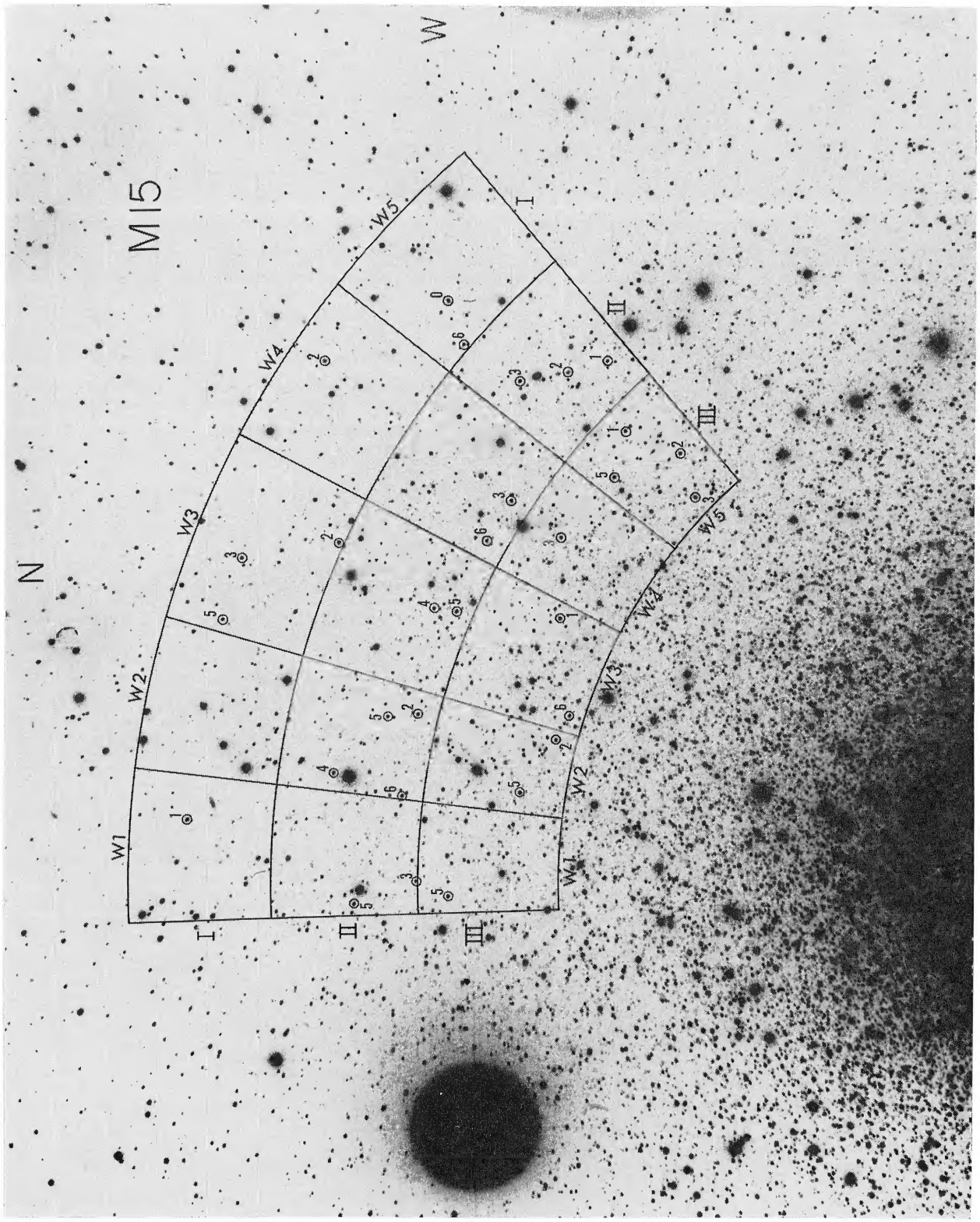

FIG. 10.—Faint stars measured photographically in M15 and listed in Table 7. Yellow plate was taken with the 200-inch on 103a-D + GG11. Called M15 Chart 4 in the tables.

SANDAGE (*see* page 847)

TABLE 5

M15 PHOTOMETRY OF CLUSTER MEMBERS

			Photoelectric							Photographic			
						n(V,B-V)		n(U-B)					
Star	Chart	Sector	V	B-V	U-B	100	200	100	200	V	B-V	U-B	n
II-75	1	II	13.00	+1.24	+0.79	3	..	1	..	13.01	+1.26	+0.98	63,61,39
S6	1	I	13.40	+1.19	+0.83	3	..	2	..	13.35	+1.21	+0.84	"
X5	1,2,3	II	13.72	+1.02	+0.58	1	..	1	..	.....	.....	.....	.....
X6	1,2,3	II	14.11	+1.01	+0.45	1	..	1	..	.....	.....	.....	.....
P13	1,2	II	14.32	+0.97	+0.43	5	18	5	18	14.32	+0.98	+0.40	63,61,39
S36	1	II	14.39	+0.91	+0.40	2	..	1	..	14.38	+0.91	+0.38	"
X2	2,3	...	14.62	+0.97	+0.40	1	..	1	..	.....	.....	.....	.....
S11	1	II	14.68	+0.88	+0.28	3	..	1	..	14.64	+0.93	+0.28	63,61,39
P6	1	II	14.93	+0.90	+0.21	3	..	1	..	14.95	+0.90	+0.24	"
A	2	...	15.05	+0.76	+0.24	..	1	..	1	15.05	+0.71	+0.29*	5,5,-
S37	1	III	15.33	+0.82	+0.26	2	..	1	..	15.27	+0.83	+0.17	63,61,39
P11	1,2	II	15.41	+0.83	+0.21	2	20	2	20	15.42	+0.82	+0.20	"
P7	1	II	15.62	+0.82	+0.19	2	..	1	..	15.59	+0.79	+0.21	"
P1	1	II	15.71	+0.79	+0.09	3	..	1	..	15.71	+0.80	+0.12	"
D	2	...	15.73	+0.74	+0.16	..	1	..	1	15.74	+0.80	+0.09*	5,5,-
IV-108K	1	IV	(15.87	+0.22	+0.13)	..	1	..	1	15.89	+0.24	.....	10,10,-
I-135K	1	I	(15.91	+0.18	+0.12)	..	1	..	1	16.12	+0.13	.....	10,10,-
IV-19K	1	IV	(15.93	+0.17	+0.15)	..	1	..	1	15.96	+0.18	.....	10,10,-
IV-68K	1	IV	(15.95	+0.23	+0.22)	..	1	..	1	15.95	+0.18	.....	10,10,-
P4	1	I	15.98	+0.17	+0.16	..	4	..	4	16.00	+0.18	+0.20	63,61,39
I-50K	1	I	(16.05	+0.12	+0.25)	..	1	..	1	15.98	+0.12	.....	10,10,-
IV-25K	1	IV	(16.06	+0.10	+0.18)	..	1	..	1	16.07	+0.06	.....	10,10,-
IV-17K	1	IV	(16.06	+0.11	+0.11)	..	1	..	1	16.07	+0.06	.....	10,10,-
I-20K	1	I	(16.08	+0.17	+0.23)	..	1	..	1	16.06	+0.15	.....	10,10,-
P3	1	II	16.09	+0.79	+0.09	4	..	2	..	16.28	+0.75	+0.06	63,61,39
IV-4K	1	IV	(16.11	+0.12	+0.20)	..	1	..	1	16.02	+0.17	.....	10,10,-
III-156K	1	III	(16.28	+0.09	-0.02)	..	1	..	1	16.43	+0.08	.....	10,10,-
P8	1	II	16.38	+0.74	+0.12	2	2	1	2	16.37	+0.78	+0.12	63,61,39
AB	2	...	16.50	+0.76	+0.08	..	1	..	1	.....	.....	.....	.....
Y	2	...	16.54	+0.78	+0.14	..	1	..	1	.....	.....	.....	.....
I-95K	1	I	(16.59	0.00	-0.32)	..	2	..	2	16.56	+0.07	.....	10,10,-
I-198K	1	I	(16.64	-0.01	-0.32)	..	2	..	2	16.58	-0.01	.....	10,10,-
III-W2-3	2	...	16.67	+0.01	-0.12	..	3	..	3	.....	.....	.....	.....
AC	2	...	16.69	+0.75	+0.08	..	1	..	1	.....	.....	.....	.....
I-73K	1	I	(16.76	-0.04	-0.28)	..	1	..	1	16.72	+0.02	.....	10,10,-
P12	1	I	16.76	+0.80	+0.07	3	2	1	2	16.80	+0.76	+0.07	63,61,39
P9	1	II	16.84	-0.01	-0.29	3	5	1	5	16.83	+0.02	-0.44	"
W	2	...	16.92	+0.71	+0.01	..	1	..	1	.....	.....	.....	.....
I-W5-4	2	...	17.21	-0.04	-0.50	..	4	..	4	17.31:	-0.09:	-0.55*	5
I-112K	1	I	(17.24	-0.05	-0.42)	..	2	..	2	16.91	+0.26	.....	10,10,-
AD	2	...	17.46	-0.08	-0.50	..	1	..	1	17.47	-0.06	-0.53*	5
N	2	...	17.64	+0.67	-0.01	..	1	..	1	17.74	+0.64	-0.08*	"
AJ	2	...	17.78	+0.68	+0.01	..	1	..	1	17.65	+0.68	+0.14*	"
III-W3-3	?		18.24	-0.07	-0.67	..	2	..	2	18.29	-0.13	-0.66*	"
AE	2	...	18.60	+0.52	-0.18	..	1	..	1	18.59	+0.56	-0.21*	"
U	2	...	18.63	+0.55:	-0.08	..	2	..	2	18.58	+0.58	-0.06:*	"
II-W4-1	2	...	18.80	+0.52	-0.08	..	1	..	1	18.84	+0.52	-0.12*	"
E†	2	...	18.80	+0.47	-0.15	..	2	..	2	18.82	+0.435	-0.13*	10
III-W2-5†	2	...	18.86	+0.53	-0.18	..	1	..	1	18.83	+0.43	-0.05*	5
A15†	2	...	18.91	+0.41	-0.02	..	1	..	1	18.92	+0.43	-0.05*	10
I-W2-1†	2	...	19.02	+0.48	-0.10	..	1	..	1	19.04	+0.44	-0.08*	5
II-W2-1	2	...	19.07	+0.39	-0.11	..	1	..	1	18.91	+0.53	-0.09*	"
Q	2	...	19.16	+0.47	-0.11	..	1	..	1	19.13	+0.49	-0.10*	"
J	2	...	19.55	+0.49	-0.11	..	1	..	1	19.54	+0.495	-0.11*	10
B6	2	...	19.55	+0.49	-0.01:	..	1	..	1	19.58	+0.515	-0.06:*	"
B3	2	...	20.02	+0.71	-0.17:	..	1	..	1	20.15	+0.60	-0.09*	"
A16	2	...	20.59	+0.62	-0.23	..	1	..	1	20.66	+0.655	-0.33*	"
A5	2	...	20.68	+0.58	+0.04	..	1	..	1	20.50	+0.77	+0.13*	"
A1	2	...	20.69	+0.64	-0.01:	..	2	..	1	20.68	+0.67	-0.12*	"
B7	2	...	20.70	+0.46	.....	..	1	..	..	20.56	+0.58	.....	"
B8	2	...	20.74	+0.28	.....	..	1	..	..	20.41	+0.615	.....	"
A6	2	...	20.70	+0.34	-0.09	..	1	..	1	20.49	+0.655	-0.15*	"
B5	2	...	20.76	+0.84	.....	..	1	..	..	20.86	+0.735	.....	"
A7	2	...	20.96	+0.87	.....	..	1	..	..	20.96	+0.715	.....	"
A8	2	...	21.15	+0.82	+0.17	..	2	..	1	21.18	+0.75	+0.21*	"
A18	2	...	21.58	+0.70	.....	..	1	..	..	21.39	+0.80	.....	"
C1	2	...	21.65	+0.97	.....	..	1	..	..	21.73	+0.83	.....	"
A17	2	...	21.69	+1.03	.....	..	1	..	..	21.58	+1.00	.....	"
A11	2	...	22.01	+0.58	.....	..	1	..	..	22.04	+0.75	.....	"

* Value of U-B is U_{pe}-B_{pg}

† These four stars are possible blue stragglers

TABLE 6

PHOTOELECTRIC DATA OF FIELD STARS NEAR M15

Star	Chart	V	$B-V$	$U-B$	n
+11°4578	1,2,3	7.64	0.54	−0.03	4H
X11	3	10.42	0.53	+0.01	2H
X8	3	10.62	0.91	+0.44	1H
X9	3	11.15	1.11	+0.76	1H
S5	1	12.87	0.78	+0.34	3H, 1S
X20	3	13.30	0.60	−0.06	1H
X30	3	13.42	0.64	+0.16	1H
X7	1,2,3	13.50	0.76	+0.24	1H
X4	3	13.65	0.57	+0.01	1H
X15	3	13.69	1.26	+1.37	2H
X19	3	13.73	0.90	+0.62	1H
X12	3	13.92	0.88	+0.48	1H
X1	3	14.01	0.63	+0.12:	1H
P5	1	14.02	0.73	+0.22	3H
P8′	1	14.47	1.00	+0.74	1H, 1S
P14	1	14.82	0.82	+0.44	2P, 2H
B	2	14.84	1.15	+0.98	3P
X10	3	15.02	0.72	+0.09	1H
X13	3	15.18	1.21	+1.21	1H
P15	1	15.42	1.34	+1.20	1P, 3H
P10	1	16.26	0.84	+0.34	1P, 3H
F	2	16.27	0.85	+0.49	1P
P2	1	16.47	0.96	+0.53	1P, 3H
AI	2	16.56	0.76	+0.27	1P
AH	2	16.61	0.90	+0.51	1P
K	2	16.69	1.12	+1.01	1P
X	2	16.72	1.12	+1.00	1P
I	2	16.95	1.03	+1.04	1P
H	2	17.32	0.62	+0.02	1P
V	2	17.35	0.64	+0.01	1P
AA	2	17.41	1.40	+1.30	1P
Z	2	17.63	1.21	...	1P
A12	2	17.71	0.80	+0.29	1P
R	2	17.79	1.19	+0.78	1P
AG	2	17.99	0.57	+0.02	1P
M	2	18.06	0.92	+0.60	1P
A14	2	18.39	1.05	+0.68:	3P
P	2	18.42	0.55	+0.08	1P
A2	2	18.58	0.86	+0.44	1P
A13	2	18.77	0.56	+0.01	1P

TABLE 7*

PHOTOGRAPHIC VALUES FOR M15 STARS NEAR MAIN-SEQUENCE TURNOFF BASED ON FIVE 200-INCH PLATES IN B AND IN V

Star	V	$B-V$	Star	V	$B-V$
I-W1-1	18.88	0.45	II-W4-3	19.25	0.51
I-W3-2	18.63	0.53	II-W4-6	19.48	0.52
I-W3-3	19.12	0.47	II-W5-1	19.31	0.51
I-W3-5	19.48	0.47	II-W5-2	19.31	0.58
I-W4-2	18.94	0.46	II-W5-3	18.85	0.51
I-W5-0	18.66	0.56	III-W1-5	19.07	0.50
I-W5-6	19.08	0.49	III-W2-2	19.08	0.48
II-W1-3	19.81	0.49	III-W2-6	18.72	0.52
II-W1-5	19.29	0.41	III-W3-1	18.76	0.55
II-W2-2	18.91	0.50	III-W3-6	19.41	0.49
II-W2-4	19.24	0.49	III-W4-3	19.23	0.49
II-W2-5	19.40	0.45	III-W5-1	18.84	0.51
II-W2-6	18.88	0.42	III-W5-2	18.85	0.52
II-W3-4	19.35	0.49	III-W5-3	18.89	0.51
II-W3-5	18.81	0.54	III-W5-4	18.99	0.52

* Stars identified in M15 chart 4 of this paper.

The measured value of $E(B - V) = 0.12$ (Sandage 1969*a*) is used to plot the diagram with reddening-free values on the assumption that $A_V = 3E(B - V)$. Large circles denote photoelectric data from Table 5, in which the photographically smoothed values fainter than $V = 18$ are used. Small dots near the main-sequence knee are from Table 7; small dots on the red edge of the horizontal branch are from Table 8. The lines drawn to represent the giant and asymptotic branches are based on the more complete photographic data of Table 8, which have not been individually plotted.

Four blue stragglers may exist, as shown by the open circles above the main-sequence turnoff. These stars are marked by daggers in Table 5, and their ultraviolet excess is discussed in § III.

d) M92

Photoelectrically calibrated photometry in M92 has been published by Arp *et al.* (1953), with additional calibration by Baum (1952). New data on the *UBV* system

TABLE 8 †, ‡

PHOTOGRAPHIC PHOTOMETRY FOR M15 STARS MEASURED IN THE RR LYRAE PROGRAM

Star	V	B-V	U-B	Branch	Star	V	B-V	U-B	Branch
P1*	15.71	0.80	+0.12	B	S37*	15.27	0.83	+0.17	B
P2*	16.42	1.00	+0.12:	F	S38	16.92	0.77	+0.02	B
P3*	16.28	0.75	+0.06	B					
P4*	16.00	0.18	+0.20	D	I-1	15.97	0.11	+0.07	D
P5*	14.07	0.66	+0.23	F	4	15.87	0.21	+0.18	D
P6*	14.95	0.90	+0.24	B	7	15.65	0.55	+0.07	H
P7*	15.59	0.79	+0.21	B	9	15.93	0.16	+0.12	D
P8*	16.37	0.78	+0.12	B	11	15.89	0.17	+0.14	D
P8'*	14.47	1.01	+0.72	F	14	16.02	0.12	+0.09	D
P9*	16.83	0.02	-0.44	D	38	14.24	0.94	+0.33	C
P10*	16.22	0.84	+0.32	F	42	16.52	-0.04	-0.19	D
P11*	15.42	0.82	+0.20	B	43	13.83	1.03	+0.50	C
P12*	16.80	0.76	+0.07	B	51	15.80	0.27	+0.22	D
P13*	14.32	0.98	+0.40	B	54	15.86	0.22	+0.18	D
P14*	14.89	0.85	+0.37	C	58	15.88	0.20	+0.20	D
P15*	15.37	1.48	+1.30	F	61	15.76	0.82	+0.10	B
					72	15.19	0.75	+0.15	C
S1	13.02	1.20	+0.94	C					
S2	15.86	0.18	+0.13	D	II-10	16.06	0.10	-0.09	D
S3	13.45	1.09	+0.70	C	11	15.81	0.20	+0.16	D
S4	12.69	1.37	+1.29	A	23	15.78	0.22	+0.15	D
S5*	12.90	0.65	+0.34	F	24	15.62	0.57	+0.04	H
S6*	13.35	1.21	+0.84	A	36	15.95	0.13	+0.12	D
S7	13.54	1.08	+0.66	C	53	16.46	0.72	+0.07	B
S8	13.41	1.09	+0.79	C	54	15.83	0.23	+0.17	D
S9	15.67	0.80	+0.17	B	59	15.87	0.21	+0.17	D
S10	15.92	0.17	+0.19	D	63	16.53	0.74	+0.04	B
S11	14.64	0.93	+0.28	A	64	13.48	1.12	+0.76	C(A?)
S12	15.89	0.79	+0.08	B	73	15.89	0.19	+0.18	D
S13	16.51	0.74	+0.04	B	74	15.95	0.15	+0.13	D
S16	15.96	0.14	+0.26	D	75*	13.01	1.26	+0.98	A
S17	16.36	0.77	+0.12	B	76	15.55	0.82	+0.18	B
S18	16.84	-0.09	-0.60	D					
S19	14.76	0.96	+0.32	A	III-15	15.87	0.17	+0.16	D
S20	15.41	0.95	+0.42	F	28	15.68	0.58	+0.09	H
S21	16.11	0.12	+0.18	D	43	15.83	0.21	+0.20	D
S22	15.42	0.86	+0.23	B	52	15.82	0.22	+0.21	D
S23	14.01	1.04	+0.68	A	67	15.93	0.17	+0.20	D
S24	15.40	0.86	+0.23	B	71	15.51	0.65	+0.09	H
S27	15.42	0.83	+0.23	B					
S28	16.42	0.79	+0.12	B	IV- 2	15.84	0.21	+0.19	D
S29	16.45	0.77	+0.15	B	31	14.84	0.93	+0.25	A(C?)
S30	14.84	0.92	+0.26	A	44	15.79	0.25	+0.18	D
S31	16.11	0.07	+0.06	D	45	15.64	0.63	+0.06	H
S32	16.59	0.73	+0.11	B	46	15.52	0.84	+0.20	B
S33	16.84	0.75	+0.07	B	63	16.06	0.08	+0.09	D
S34	16.99	0.76	+0.01	B	66	15.95	0.15	+0.15	D
S35	16.80	0.78	+0.10	B	68	15.77	0.24	+0.17	D
S36*	14 38	0.91	+0.38	C					

† Tabulated values are means from 63 plates in V(103a-D + GG11), 61 plates in B(103a-O + GG13), and 39 plates in U(103a-O + UG2) taken with 100-inch diaphragmed to 58 inches. Measurements and reductions by Sandage, Sandage, Katem, and Breuckel (unpublished).

‡ Stars in this table are identified on M15 CHART 1.

* Photoelectric standard. See Tables 5 and 6.

were published to $V = 16$ by Sandage and Walker (1966), and additional horizontal-branch stars were measured in the present program, and are discussed elsewhere (Sandage 1969*a*).

To avoid unnecessary duplication, we list in Table 9 only those stars measured in the present study which have not been previously published. The random probable errors in Table 9 average 0.02 mag in each color for V brighter than 20, and are approximately double this for V fainter than 20.

Extensive smoothing of the data was done by Katem from measurements of seven 200-inch plates in B and in V brighter than $V = 18.6$, and from the same plates measured twice for the fainter stars. The smoothed values are listed in the second part of Table 9; they constitute the adopted data for the main sequence. No ultraviolet plates were obtained, but partial smoothing of $U - B$ was again done by taking the smoothed B_{pg}

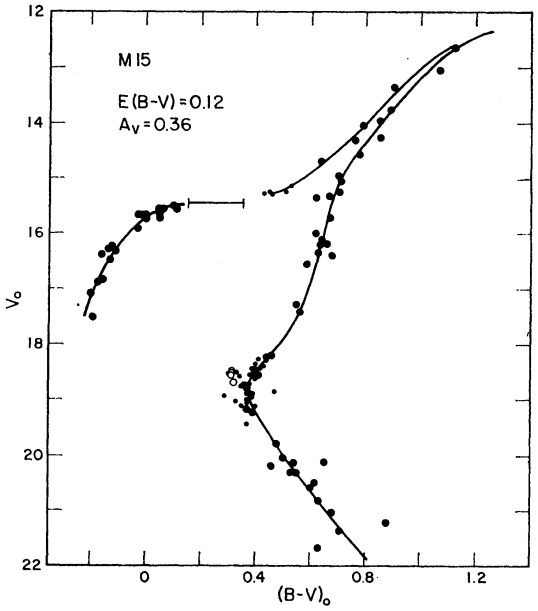

FIG. 11.—C-M diagram for M15 corrected for $E(B - V) = 0.12$, and $A_v = 0.36$ mag. *Large filled circles*, photoelectric or photographic values from Table 5; *small circles*, photographic values from Tables 7 and 8; *open circles*, possible blue stragglers listed in Table 5.

and forming $U_{pe} - B_{pg}$, as listed in the penultimate column. All stars in Table 9 are marked in Figure 12 (Plate 13). The identification scheme via sectors is evident.

The C-M diagram for M92 is shown in Figure 13. The large dots brighter than $V = 18.50$ are photoelectric as measured; fainter than this, the photographically smoothed values from Table 9 are plotted. Six stars carried in the photographic work but not measured photoelectrically (Table 9, end of the *member* section) are shown as small circles. Data which are plotted but not listed in Table 9 are from Sandage and Walker (1966) and Sandage (1969*a*).

III. THE TWO-COLOR DIAGRAM

The ultraviolet excess for globular-cluster stars was found in NGC 4147 (Sandage and Walker 1955), and was shown to be a general feature of halo clusters by data from later studies in M3 (Johnson and Sandage 1956), M13 (Arp and Johnson 1955 if their $E(B - V) = 0.12$ is replaced by 0.03), M5 (Arp 1959), and in many clusters studied subsequently. That it is an index of metal abundance is clear from (1) Arp's (1964, Table 3) correlation of $\delta(U - B)$ with the Deutsch (Kinman 1959) and Morgan (1959)

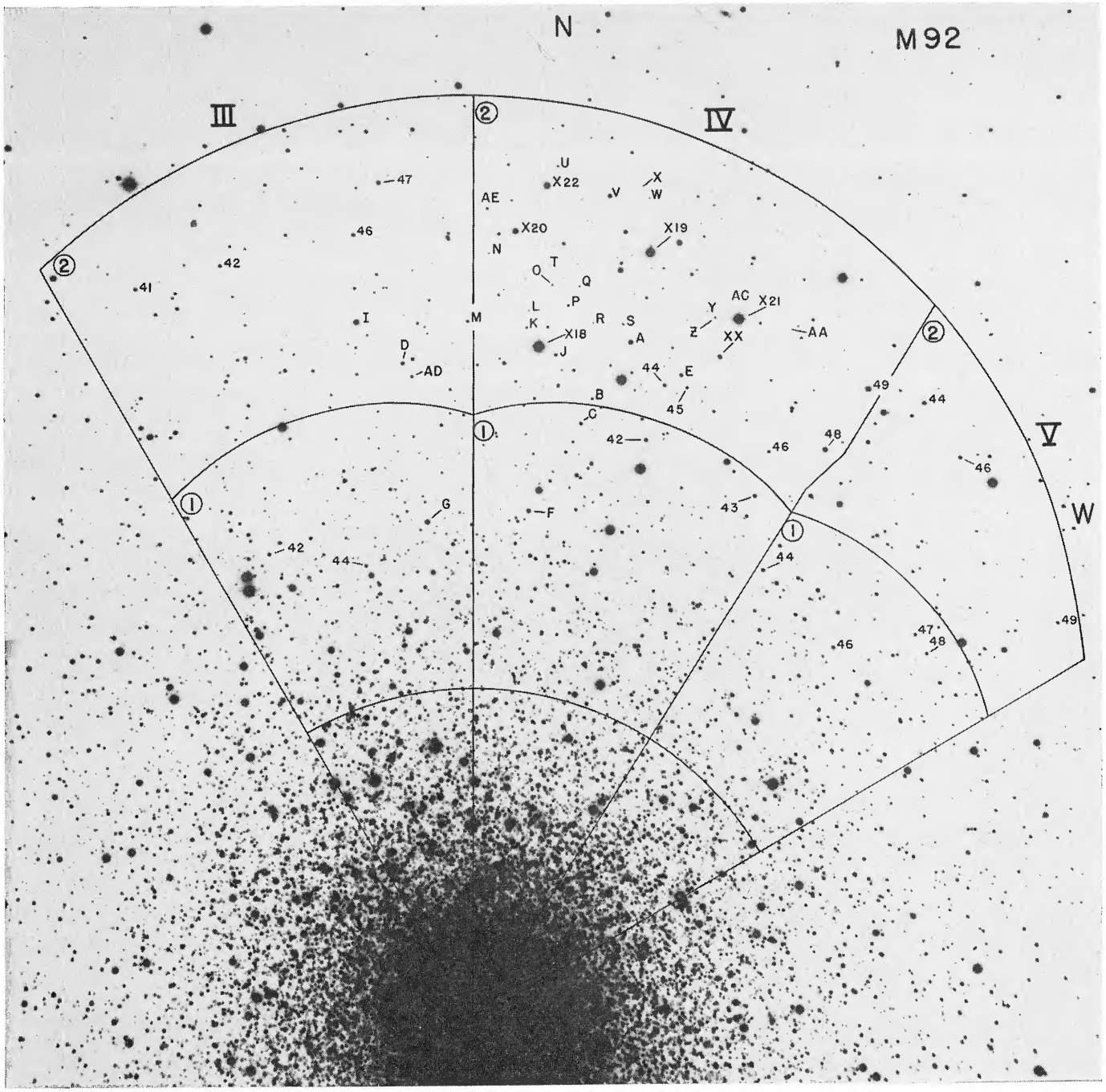

FIG. 12.—Chart of the faint stars in M92 listed in Table 9 from a blue plate taken with the 200-inch on 103a-O + GG13

SANDAGE (*see* page 851)

metal types, and (2) the abnormally small $\delta(U-B)$ for stars in the known metal-rich cluster NGC 6171 (Sandage and Katem 1964; Dickens 1971).

Wallerstein and Helfer (1966) have given a preliminary calibration of $\delta(U-B) = f[\mathrm{Fe/H}]$ for K giants which shows that $\delta(U-B)$ changes very slowly for $[\mathrm{Fe/H}] < -1$. Consequently, observations must be very precise and the reddening known with great accuracy if small differences in [Fe/H] are to be found by this phototometric method. Nevertheless, $\delta(U-B)_{\mathrm{giant}}$ provides the only data known for some clusters.

Figure 14 shows the two-color diagram for the four clusters studied here, plotted from data either listed or referenced in § II. No reddening corrections have been applied to M3, M13, or M92; but $E(B-V) = 0.12$, $E(U-B) = 0.08$ have been applied to M15. In inspecting the diagrams one must therefore remember to apply small (or zero) corrections to the first three clusters depending on which reddening values the reader

TABLE 9 *

M92 PHOTOELECTRIC STANDARDS FAINTER THAN V=16.26

		Photoelectric Values				Photographic Values			
Sector	Star	V	B-V	U-B	n (200)	V	B-V	$U_{pe}-B_{pg}$	n
III-2	I	16.26	0.65	-0.05	2	16.27	0.64	.....	7
IV-2	49	16.35	0.64	0.00	1	16.37	0.64	.....	"
IV-2	48	16.61	0.69	-0.03	1	16.66	0.63	.....	"
IV-2	A	17.01	0.62	-0.11	2	17.01	0.62	.....	"
IV-1	F	17.38	0.61	-0.16	2	17.40	0.60	.....	"
V-2	44	17.65	0.64	-0.19	1	17.73	0.56	.....	"
IV-2	V	17.84	0.50	-0.16	1	17.79	0.58	-0.19	"
V-2	46	17.93	0.75	.....	1	18.01	0.75	.....	"
IV-1	42	17.94	0.49	.....	1	17.96	0.51	.....	"
III-2	D	18.22	0.40	-0.15	3	18.25	0.41	-0.19	"
V-1	46	18.27	0.46	-0.14	2	18.28	0.46	-0.15	"
IV-2	E	18.24	0.405	-0.18	2	18.24	0.45	-0.23	"
III-2	46	18.27	0.41	-0.21	1	18.29	0.40	-0.22	"
III-1	42	18.30	0.43	-0.24	1	18.17	0.43	(-0.11)	"
III-2	41	18.39	0.38	-0.15	1	18.53	0.32	-0.23	"
III-2	42	18.40	0.37	.....	1	18.52	0.32	.....	"
IV-2	44	18.63	0.40	-0.12	1	18.59	0.45	-0.13	"
IV-2	J	18.71	0.47	-0.25	1	18.73	0.425	-0.22	14
IV-1	C	18.78	0.36	-0.20	1	18.63	0.39	-0.08	"
IV-2	46	18.89	0.44	.....	1	18.92	0.41	.....	"
IV-2	45	18.92	0.41	.....	1	18.94	0.44	.....	"
IV-2	P	19.24	0.53	-0.30	1	19.30	0.47	-0.30	"
III-2	AD	19.35	0.45	-0.24	1	19.33	0.395	-0.16	"
IV-2	K	19.88	0.44	-0.23	1	19.87	0.53	-0.31	"
IV-2	U	19.95	0.64	-0.30	1	19.94	0.57	-0.22	"
IV-2	Z	19.95	0.64	-0.06	1	20.04	0.62	-0.13	"
IV-2	S	20.01	0.50	.....	1	19.98	0.56	.....	"
IV-2	R	20.28	0.47	0.02	1	20.26	0.72	-0.21	"
IV-2	O	20.40	0.34	-0.24	1	20.11	0.57	-0.18	"
IV-2	L	20.49	0.61	-0.17	1	20.56	0.63	-0.26	"
IV-2	Y	20.56	0.38:	+0.03:	1	20.54	0.66	-0.23	"
IV-2	N	20.59	0.70	-0.28	1	20.56	0.61	-0.16	"
IV-2	W	20.80	0.18	.....	1	20.71	0.58	.....	"
IV-2	AC	21.03	0.80	.....	1	21.23	0.81	.....	"
IV-2	T	21.07	0.53	.....	1	20.94	0.73	.....	"
IV-2	AA	21.39	1.14	.....	1	21.48	0.98	.....	"
IV-2	AE	21.40	1.02	.....	2	21.40	0.95	.....	"
IV-2	X	22.26	0.82	.....	1	22.11	0.91	.....	"
III-2	47	.....	.....	.....	..	17.52	0.61	.....	"
IV-1	43	.....	.....	.....	..	18.02	0.50	.....	"
III-1	44	.....	.....	.....	..	18.90	0.37	.....	"
V-1	48	.....	.....	.....	..	18.92	0.42	.....	"
III-2	M	.....	.....	.....	..	18.99	0.41	.....	"
V-2	49	.....	.....	.....	..	19.06	0.41	.....	"
		Field Stars With V > 16.70							
III-1	G	16.70	0.26	0.24	1	.....	.....	.....	..
IV-2	XX	17.40	0.73	0.15	1	.....	.....	.....	..
V-1	44	18.06	0.49	-0.07	1	18.08	0.46	-0.06	14
IV-2	B	18.78	1.20	1.31	1	.....	.....	.....	..
IV-2	Q	19.60	1.19	.....	1	.....	.....	.....	..

*Additional M92 stars measured photoelectrically in this program were published by Sandage and Walker (Ap. J. 143, 313, 1966 for giants, horizontal branch, and field stars), and by Sandage (Ap. J. 157, 515, 1969, Table 6 for horizontal branch stars).

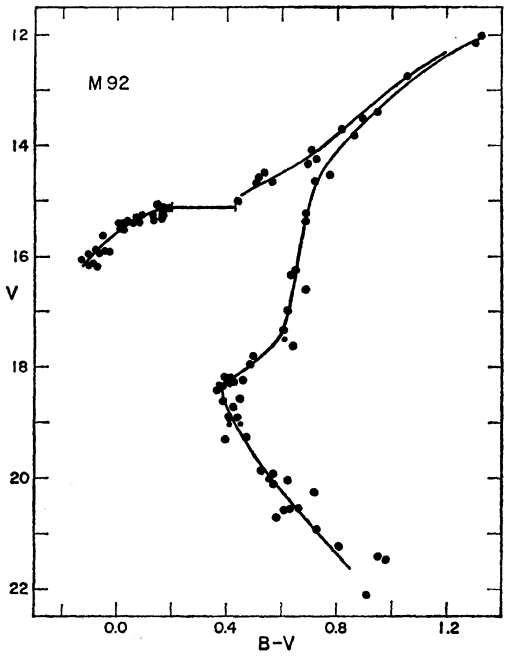

FIG. 13.—C-M diagram for M92 from the sources listed in the text. No corrections for reddening or absorption have been applied.

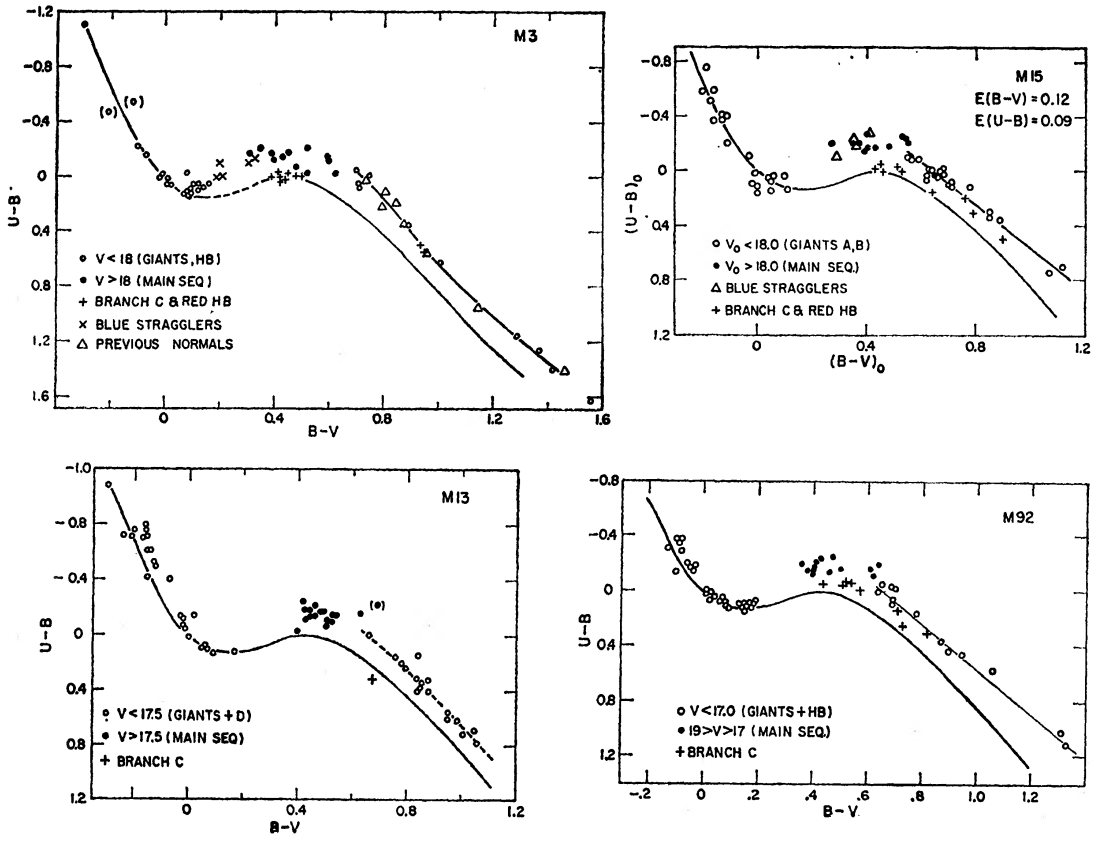

FIG. 14.—Composite two-color diagrams for M3, M13, M15, and M92 showing stars from different parts of the C-M diagram. Corrections for reddening have been applied only for M15.

wishes to adopt (Sandage 1964, 1969*a;* McNamara and Langford 1969; Crawford and Barnes 1969; McClure and Racine 1969). In any case, the corrections are small, lying between $0.00 \leq E(B - V) \leq 0.03$ according to these authors.

Stars from various parts of the H-R diagram differ in their $U - B$ excess, according to various combinations of temperature, line blanketing, and surface gravity. In the following paragraphs, we discuss each part of the diagram separately.

a) Blue End of the Horizontal Branch

Stars with $(B - V)_0 < 0.2$ lie close to the luminosity class V main sequence (plotted from Eggen 1965). The result is expected from the atmospheric models of Mihalas (1966), and is observed in other clusters besides those studied here (see, e.g., Eggen 1960; Newell 1970). Previous suggestions (Arp and Johnson 1955 for M13; Arp 1962 for M5) that stars bluer than $(B - V)_0 = -0.10$ have a large ultraviolet deficiency relative to the class V line are not confirmed. To make certain of this point a special effort was made to measure the fainter horizontal-branch stars in M13 bluer than $(B - V)_0 = -0.1$, which is where the large deficiency was previously seen.

The most important stars to check were those from Table 2 of Arp and Johnson (1955) for which the abnormally blue $B - V$ colors of ~ -0.4 were listed. Stars 63 and 127 were crowded, which precluded photoelectric measurements. Stars 105, 110, and 122 could be measured reliably, although extensive background mapping of the neighborhood was necessary. The data, given elsewhere (Sandage 1969*a*, Table 3), showed redder $B - V$ colors of ~ -0.2 which removes the deficiency. To test the result further, eighteen other faint horizontal-branch stars in M13 identified by Savedoff (1956) far from the cluster center were measured, as listed elsewhere with S numbers (Sandage 1969*a*, Table 3), and the results are shown in Figure 14. No evidence for the deficiency is present.

To be more certain of the result, a special search was made for very faint horizontal-branch stars in M15 (Sandage *et al.* 1968), and these were measured with the 200-inch in the 1967 observing season. The stars are listed in Table 5 and are designated by K after the ordinary number. Figure 14 shows the result for M15. The data for M92 are also consistent with the conclusions of no deficiency, although few stars exist bluer than $B - V = -0.10$.

However, the situation appears to be different for redder horizontal-branch stars. A small $U - B$ deficiency seems to exist in M15 near $(B - V)_0 = 0.0$, similar to that found in NGC 6397 and ω Cen by Newell, Rodgers, and Searle (1969*a*, *b*), and in M5 by Arp (1962). An explanation in terms of deblanketing, differences in surface gravity, and Mihalas's (1966) model atmospheres has been given by Newell (1970).

b) Red End of the Horizontal Branch, and the Asymptotic Branch C

The C-M diagrams for M3 (Fig. 4) and M15 (Fig. 11) show a number of stars on the red end of the horizontal branch. The present photometry of M92 (Fig. 13) contains one such star, and several on the asymptotic branch C. It has been known for some time that these stars have either no ultraviolet excess or only a slight one relative to the Hyades fiducial color-color line. The explanation is that the fiducial line for stars of low surface gravity (but which have Hyades-like abundances) passes *below* the class V relation in the range $0.2 < (B - V) < 1.0$ (e.g., Johnson and Morgan 1953, Fig. 8; Eggen and Sandage 1964, Fig. 4). Deblanketing from this line due to low metal abundance nearly compensates for the gravity effect, and the cluster stars appear close to the Hyades line by accident. This *apparent* absence of an ultraviolet excess for horizontal-branch stars, together with its presence in F–G subdwarfs, provides a powerful photometric method of finding such F–G giants among high-velocity stars in the field.

One asymptotic-branch star redder than $(B - V)_0 = 0.6$ has been measured in M13, and four such stars have been measured in M15. Figure 14 shows that stars on branch C have a smaller $\delta(U - B)$ than giants at the same $B - V$. The effect is the same as

previously found in M92 (Sandage and Walker 1966) and in ω Cen (Geyer 1967). Although no satisfactory explanation has yet been adopted, it may not be out of the question that enrichment of the surface by metals from the interior has occurred by mixing in an evolutionary stage during which there was predominant convection.

c) The Giant (A) and Subgiant (B) Branches

Giants and subgiants redder than $B - V = 0.5$ are shown as open circles in Figure 14. The $U - B$ excess, read at $(B - V)_0 = 1.0$, is largest for M15 and M92, intermediate for M3, and smallest for M13. Although the differences are not large and the sample is rather small, the sense of the $\delta(U - B)$ variation agrees with spectroscopic evidence that M13 has stronger lines than M15 and M92, with M3 intermediate. The results are summarized in the unnumbered table below.

Cluster	$E(B-V)$	$\delta(U-B)_{B-V=1.0}$	Deutsch Type	Morgan Type
M13.....	0.03	0.15	A	III
M3.....	0.00	0.18	AB	II
M92.....	0.02	0.26	C	I
M15.....	0.12	0.28	C	I

The excess among the giants continues to very red colors. Not plotted in Figure 14 is a member of M13 at $B - V = 1.57$, $U - B = 1.81$ which shows $\delta(U - B) = 0.07$ relative to the standard giant line. The fact that the guillotine acting on $\delta(U - B)$ for giants is not as strong as that for dwarfs must mean that the slope of the blanketing line is steeper for giants in the range $(B - V) \gtrsim 1.0$.

d) Blue Stragglers

There has always been a question of whether the many blue stars found above the M3 main sequence (Sandage 1953, Fig. 1) are cluster members. If they are, then this cluster is abnormal in its population of blue stragglers. A necessary condition for membership is the presence of an ultraviolet excess. Most of the known stars are too close to the cluster center for reliable photoelectric measurement. However, five of the sample (I-V-6, I-III-36, II-I-74, II-II-51, and II-III-9) were marginally distant enough to measure, as given in Table 1 and plotted as crosses in Figure 14, M3. All have an ultraviolet excess of $\delta(U - B) \simeq 0.15$ mag, which is close to what is expected for luminosity class V stars in this color range. Therefore, the stars may be cluster members. One additional star near the turnoff (F5 with $V = 18.94$, $B - V = 0.35$, $U - B = -0.20$ from Table 1, and $V = 18.99$, $B - V = 0.41$, $U - B = -0.27$ by Johnson and Sandage 1956) may also be a straggler (see Fig. 4) if its color is as blue as $B - V = 0.35$.

Four highly probable stragglers exist in M15 with $(B - V)_0 \simeq 0.31$ (E, III-W2-5, A15, and I-W2-1; see Table 5 and Fig. 11). They are plotted as triangles in Figure 14, and all show a large ultraviolet excess.

e) The Main Sequence

Stars near the main-sequence turnoff are plotted as filled circles in Figure 14 for all four clusters. The main-sequence data are the least accurate in this diagram due to the extreme faintness of the stars. Where available, the partially smoothed $U_{pe} - B_{pg}$ values are plotted. The largest excess is for M15, followed by M92, then M13, with M3 having the smallest $\delta(U - B)$. It is surprising that $\delta(U - B)_{d,M13} > \delta(U - B)_{d,M3}$ because there is no doubt that M13 has the higher metal abundance. The most likely explanation is that the M3 main-sequence photometry in $U - B$ is not yet precise enough. Considerably better data can now be obtained with the 200-inch pulse-counting equipment, and the problem should be reinvestigated.

Because the main-sequence photometry is so crucial in one of the methods of distance determination, we show the data in more detail in Figure 15. The lower solid line in each panel represents the Hyades fiducial line; the upper solid line is the adopted limiting relation for the maximum abundance effect (Eggen 1968, Fig. 1; Sandage 1969*b*, Table 1A). The dashed line is derived from the observed mean values as follows.

For each cluster, the data in Figure 15 were averaged to give $\langle\delta(U-B)\rangle$ at the observed average value of $(B-V)_0$. To correct for the guillotine, these were transformed to $\langle\delta(U-B)\rangle$ at the observed average value of $(B-V)_0 = 0.6$ by the precepts given elsewhere (Sandage 1969*b*, Table 1A), with the results listed in Table 10. Here, n is the weighted number of stars involved in the mean. In general, the open and closed circles were treated equally, with half-weight given to stars fainter than $V \simeq 20.5$, or which are

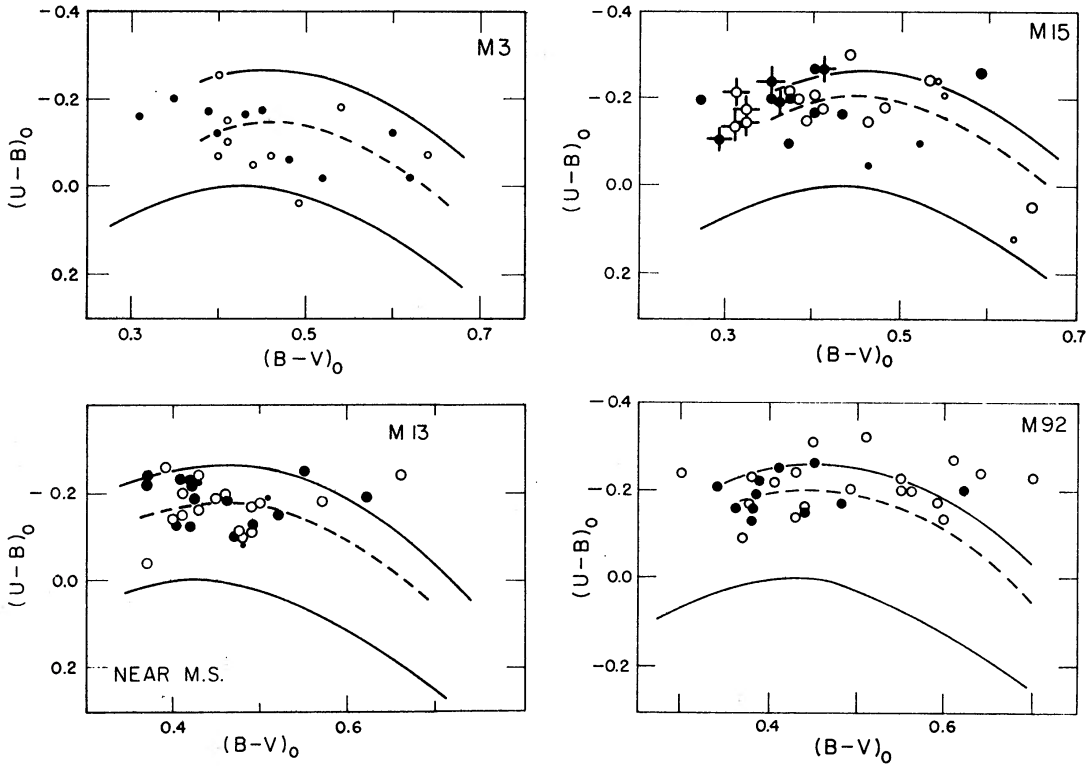

FIG. 15.—Two-color diagrams for main-sequence stars only. Closed circles used directly observed $(U-B)_{pe}$ values; open circles used the partially smoothed $U_{pe} - B_{pg}$ data. Blue stragglers from M15 are shown as flagged points. Data have been corrected for reddenings of 0.00, 0.03, 0.12, and 0.02 for M3, M13, M15, and M92.

TABLE 10

MEAN EXCESS FOR MAIN-SEQUENCE STARS

CLUSTER	OBSERVED MEAN POINT			
	n	$\langle(B-V)_0\rangle$	$\langle\delta\rangle$	$\langle\delta\rangle_{0.6}$
M3	19	0.460	0.145	0.171
M13	28	0.437	0.174	0.208
M15	14.5	0.414	0.199	0.234
M92	18	0.410	0.197	0.238

otherwise uncertain. The mean for each cluster was then used to draw the dotted lines in each panel of Figure 15.

IV. DISTANCE MODULI

Photometric methods to determine distances depend on some form of either (*a*) main-sequence fitting to some standard or (*b*) independent knowledge of $\langle M_v \rangle = f(\langle P \rangle)$ or $g(\Delta S)$ for RR Lyrae stars, where $\langle P \rangle$ is the mean period of Bailey type *ab* variables in a given cluster, and ΔS is the Preston (1959) metal index.

a) Main-Sequence Fitting

i) *The Method*

The main sequence to which a given cluster is to be fitted may differ from that of the Hyades for three reasons. (1) The position of the sequence in the (M_{bol}, log T_e)-plane is sensitive to changes in X and Z. (2) Observed colors are affected by variations in Z due to line-blanketing differences, and must be "corrected to a standard blanketing condition." (3) Even after this correction, there is no guarantee (because of point [1]) that the Hyades (M_v, $B - V$)-sequence is the correct one for the clusters.

To test point (3), we have proceeded empirically in the past (Eggen and Sandage 1962) by applying blanketing corrections (Sandage and Eggen 1959; Melbourne 1960; Wildey *et al.* 1962) to *field stars* with $\pi(\text{trig}) \geq 0''.035$ which have a range of $\delta(U - B)$ values, and then using the resulting main sequence as a standard. This procedure circumvented both point (1) and the distance to the Hyades itself, because the basic data were the parallaxes of the field subdwarfs. That the procedure is independent of the Hyades modulus was correctly pointed out by Demarque (1967*b*) and by Cayrel (1968). The point is visible in a more explicit form by the following variation of the method, which was used in this investigation.

All parallax stars used by Eggen and Sandage (1962) were retained and supplemented by more recently available data. The stars from Allegheny, Yale, and the Cape were combined, and the excess $\delta(0.6)$ was computed for each star. As before, the sample was divided into four groups according to $\delta(0.6)$, with the class intervals $0.05 \geq \delta(0.6) \geq -0.05$, 0.06–0.10, 0.11–0.15, and ≥ 0.16. Three steps were then followed.

1. A fiducial main sequence in M_v, $(B - V)_0$ was adopted such that its shape was identical with the mean shape of the *observed* main sequences in M3, M13, M15, and M92, taken from Figures 4, 6, 11, and 13. This ensures that evolutionary effects are accounted for straightaway. The adopted sequence is not listed here because it agrees with that tabulated by Eggen (1965, Table 1) in the range $1.0 > (B - V) > 0.45$. It will be evident from the next step that we could have used any other zero point for this fiducial line, as long as the shape of the line is kept the same.

2. For each star, M_v was computed using the observed V-magnitude and $\pi(\text{trig})$. This value was compared with M_v of the fiducial sequence, read at the observed $B - V$ for the star in question, and the difference $\Delta M_v \equiv M(\text{actual}) - M(\text{fiducial})$ was formed. As expected from the previous study (Eggen and Sandage 1962), ΔM_v is a strong function of $\delta(U - B)_{0.6}$. Although the effect is due to a combination of (1) blanketing and (2) variable X and Z on the (M_{bol}, log T_e)-position of the main sequence, we need not separate the two causes because only the empirical $\Delta M_v = f[\delta(0.6)]$ is used in step 3.

3. Taking means, weighted according to the inverse square of the probable error in M_v, gives the correlation shown in Figure 16 and listed in Table 11. This permits $\langle \Delta M_v \rangle$ to be read at the appropriate value of $\langle \delta(0.6) \rangle$ listed in Table 10. The modulus then follows straightaway by combining ΔM_v, the fiducial sequence, and the observed C-M diagram.

The power of the method is that no use is made of either the position of the Hyades main sequence or of blanketing corrections. Its weakness lies in the small number of field subdwarfs with $\delta(0.6) \geq 0.11$ and $\pi(\text{trig}) \geq 0''.035$ which define Figure 16.

Before the results are discussed, additional comment is required on Figure 16 and Table 11. Many stars exist in data groups A and B, and the parallaxes are in general large, averaging $\langle\pi\rangle = 0''.070$ for Group A and $0''.060$ for Group B. The small sample size of Group C (16 stars) and Group D (9 stars), together with their smaller mean parallax of $\langle\pi\rangle = 0''.050$, causes a bias in Figure 16 (Wallerstein 1967) such that the plotted ΔM_v values are too large. But, as Wallerstein emphasizes, the actual bias is smaller than in his model because (1) our sample is progressively more incomplete toward smaller π, causing the effective cutoff parallax to be larger than $0''.035$, and (2) our weighting of the individual ΔM_v values by the inverse square of the probable errors of M(trig) gives high weight to stars of large parallax, for which the bias is very small. The actual effect for our sample is hard to estimate, but Wallerstein's model calculations show it could be as large as 0.4 mag for data groups C and D, but undoubtedly smaller for groups A and B.

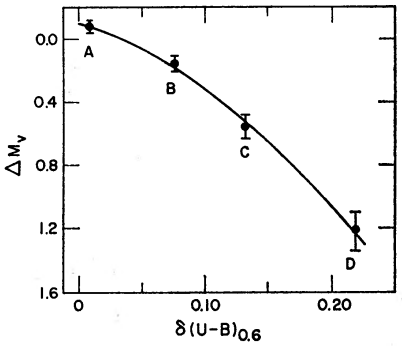

FIG. 16.—Correlation of mean magnitude difference below the adopted fiducial main sequence (Eggen 1965) and the excess $\delta(U-B)_{0.6}$ for trigonometric stars divided into excess groups A, B, C, and D.

TABLE 11

CORRELATION OF ΔM_v WITH $\delta(0.6)$ FOR FIELD SUBDWARFS

Group	$\delta(.6)$	n	$\langle\delta(.6)\rangle$	$\langle\Delta M_v\rangle$
A.....	−0.05 to +0.05	56	0.009	−0.06±0.030
B.....	+0.06 to +0.10	36	0.076	+0.17±0.043
C.....	+0.11 to +0.15	16	0.132	+0.56±0.081
D.....	≥0.16	9	0.218	+1.22±0.116

Listed in Table 12 are the individual stars in groups C and D. The photometry is taken generally from the literature. Values of $U-B$ in parentheses are on the Cape $(U-B)_c$ refractor system, from which the excess follows from Eggen (1959), Cousins, Eggen, and Stoy (1961), and Cousins and Stoy (1963). The parallaxes are from Allegheny alone for the northern stars, and from Cape plus Yale for the southern. The weights are on the system of Jenkins (1952).

To reduce the present uncertainty it will be necessary to improve the parallax data in Table 12, and to increase the sample size. Many candidates for nearby subdwarfs exist, and a concentrated parallax program will surely produce enormous dividends.

ii) *The Results*

Despite the present uncertainties, we must use Figure 16 if photometric moduli are to be obtained from the present data. The results of fitting each C-M diagram (Figs. 4, 6, 11, and 13 corrected for reddening) to the adopted fiducial main sequence and then

applying the ΔM_v correction from Figure 16 are given in Table 13. The various columns list the following: the reddening in column (2); $\langle\delta(0.6)\rangle$ from Table 10 in column (3); $(m - M)_{AV} + \Delta M_v$ in column (4), obtained by fitting directly to the fiducial main sequence; ΔM_v from Figure 16 in column (5); in column (6) the resulting modulus $(m - M)_{AV}$ found by subtracting column (5) from column (4); the observed apparent magnitude of the RR Lyrae stars in column (7); and the resulting M_v(RR) obtained from columns (6) and (7) in column (8).

Table 13 is divided into two sections. Part I uses the observed $\delta(0.6)$ values as they stand, while Part II uses modified δ values based on the positive spectroscopic (Kinman 1959; Morgan 1959) and photometric (§ III) evidence that $\delta(0.6)_{M3}$ should be greater

TABLE 12

INDIVIDUAL PARALLAX DATA FOR STARS IN EXCESS GROUPS C AND D

Yale No.	Sp Tp.	V	B-V	U-B	δ	δ(0.6)	π	W	M_V	ΔM_V
				GROUP C 0.15≥δ(.6)≥0.11						
216	G3	7.72	0.60	(1.64)	0.12	0.12	39	17	5.68 ± .45	0.90 ± .45
219	G5VI	5.16	0.70	0.10	0.15	0.16	146	16	5.98 ± .12	0.66 ± .12
1498	G0	7.11	0.62	0.00	0.15	0.15	35	16	4.83 ± .50	-0.05 ± .50
1749	F5	6.53	0.47	-0.11	0.11	0.13	38	20	4.43 ± .40	0.51 ± .40
2392	dG1	8.08	0.60	(1.63)	0.13	0.13	40	17	6.09 ± .43	1.31 ± .43
3096	G4V	7.30	0.68	(1.72)	0.12	0.13	35	20	5.02 ± .43	-0.18 ± .43
3249	dF4	5.86	0.50	(1.56)	0.12	0.13	44	17	4.08 ± .39	-0.02 ± .39
3425a	...	9.43	0.85	(1.86)	0.14	0.15	35	17	7.15 ± .50	1.05 ± .50
3669	K0V	7.51	0.82	(1.84)	0.13	0.14	70	20	6.74 ± .19	0.79 ± .19
3734	F8	7.68	0.54	(1.60)	0.11	0.12	36	19	5.46 ± .42	1.07 ± .42
3909	G2V	6.99	0.60	(1.65)	0.11	0.11	40	20	5.00 ± .38	0.22 ± .38
3943	G0V	6.96	0.58	-0.02	0.13	0.13	43	16	5.13 ± .40	0.49 ± .40
4138	G2V	6.79	0.63	0.04	0.13	0.13	52	20	5.37 ± .29	0.42 ± .29
4932	dG6	6.44	0.65	0.07	0.12	0.13	53	20	5.06 ± .29	0.04 ± .29
5009	G0V	6.52	0.58	(1.62)	0.12	0.12	48	17	4.93 ± .36	0.29 ± .36
5020	G8V	7.76	0.72	0.16	0.13	0.14	40	16	5.77 ± .43	0.34 ± .43
				GROUP D δ(.6)≥0.16						
763	F9V	6.68	0.54	-0.09	0.16	0.16	54	28	5.34 ± .24	0.94 ± .24
1857	G2VI	8.34	0.60	-0.12	0.25	0.25	41	20	6.40 ± .37	1.63 ± .37
2401	G1V	7.77	0.62	-0.02	0.17	0.17	47	20	6.11 ± .32	1.24 ± .32
2745	G8Vp	6.49	0.75	0.15	0.19	0.20	111	28	6.72 ± .12	1.12 ± .12
3211	G9	9.68	0.78	(1.80)	0.15	0.16	37	20	7.52 ± .35	1.77 ± .35
3425	G8VI	9.05	0.78	(1.75)	0.21	0.23	35	17	6.77 ± .50	1.02 ± .50
3767.0	.....	9.63	0.75	0.10	0.24	0.28	46	17	7.94 ± .37	2.34 ± .37
4524	K0V	8.84	0.85	0.34	0.20	0.26	38	20	6.67 ± .40	0.57 ± .40
5098	F6VI	7.41	0.50	-0.21	0.23	0.25	41	16	5.47 ± .42	1.37 ± .42

TABLE 13

PHOTOMETRIC MAIN-SEQUENCE FITTING
(METHOD *a* FOR DISTANCES)

Cluster (1)	$E(B-V)$ (2)	$\langle\delta(0.6)\rangle$ (3)	$(m-M)_{AV}+\Delta M_v$ (4)	ΔM_v (5)	$(m-M)^*_{AV}$ (6)	V(RR) (7)	M_v(RR) (8)
			I. Using Observed $\langle\delta(0.6)\rangle$				
M3.....	0.00	0.171	16.10±0.05	0.82	15.28	15.63	+0.35
M13.....	0.03	0.208	15.65±0.05	1.14	14.51	14.57	+0.06
M15.....	0.12	0.234	15.90±0.05	1.38	14.52*	15.50*	+0.98
M92.....	0.02	0.238	15.60±0.05	1.42	14.18	15.09	+0.91
			II. Using Adjusted $\langle\delta(0.6)\rangle$ for M3 and M13				
M3.....	0.00	0.20	16.10±0.05	1.07	15.03	15.63	+0.60
M13.....	0.00	0.18	15.40±0.05	0.88	14.52	14.57	+0.05

* Tabulated for M15 is $(m - M)_0$, not $(m - M)_{AV}$.

than $\delta(0.6)_{M13}$ due to weaker Fraunhofer lines. We have adopted $\delta(0.6)_{M3} = 0.20$ and $\delta(0.6)_{M13} = 0.18$, found by smoothing the relation between δ(giants) and δ(dwarfs) for wide binaries (Eggen and Sandage 1964, Appendix) and using δ(giants) given in § III. In Part II we also assume that $E(B - V) = 0.00$ for M13 as measured by Crawford and Barnes (1969) and McClure and Racine (1969).

iii) *Errors*

The weakness of the method is its high sensitivity to observational errors in $E(B - V)$, $\delta(0.6)$, and the observed colors of the main sequence. Errors of order $\epsilon(\langle\delta\rangle) \simeq 0.04$ mag exist in $\delta(U - B)$ (note the scatter in Fig. 15). Analysis of Figure 16 shows that this error propagates as $\epsilon(\Delta M_v) \propto 8.8\epsilon(\delta)$, which leads to random errors of $\sim$0.35 mag in M_v(RR) from this cause alone.

Errors in the reddening, or in the measured main-sequence colors, enter as 6ϵ in M_v(RR) because the equation of the main sequence is $M_v \propto 6(B - V)$ near $B - V = 0.6$. The *combined* errors $\epsilon(E)$ and $\epsilon(B - V)$ can be as large as $\sim$0.05 mag in the present material (i.e., $\pm$0.02 for $E(B - V)$ and $\pm$0.03 for $B - V$), which introduces an uncertainty of $\sim$0.3 mag in M_v(RR) from this cause.

Finally, the bias in Figure 16 introduces a systematic error which is about 0.2 mag in the sense that Table 13 values are too faint.

iv) *Adopted Values*

Neglecting the bias for the moment, we believe that the most reliable values from Table 13 are M_v(RR) = 0.60 for M3, 0.98 (M15), 0.91 (M92), and 0.05 (M13). For reasons discussed later (§ V), M13 appears to be exceptional. It may be that its few RR Lyrae stars are not on the normal horizontal branch but are rather in a later evolutionary state connected with the asymptotic branch. If so, M13 should be considered separately. Adopting this point of view gives $\langle M_v(\text{RR})\rangle = 0.83 \pm 0.15$ (A.D.) for the three remaining clusters. Correcting for a 0.2-mag bias gives a final mean of $\langle M_v(\text{RR})\rangle \simeq 0.6$, with a random uncertainty of perhaps $\pm$0.2 mag.

The result is very disappointing in one important aspect. Because M3 and M15 + M92 are of different Oosterhoff-Sawyer RR Lyrae period-groups, it is expected (Sandage 1958, 1969*a*; Christy 1966, 1968, 1969) that the RR Lyrae stars in M3 should be fainter than those in M15 and M92 by about 0.3 mag. For many years this has appeared to be the only reasonable explanation of the Oosterhoff-Sawyer phenomenon, and, in view of Christy's detailed predictions, the hypothesis is not easily given up. But the results from Table 13 show the opposite trend, with M3 [M_v(RR) = 0.60] brighter than M15 (0.98) and M92 (0.91). If the model (Sandage 1958, Figure 3) is correct, then errors must exist in Table 13 which amount to 0.60 mag for M3, or a combination of errors for all three clusters which accumulate to $\sim$0.6 mag.

Because the Oosterhoff-Sawyer phenomenon is such an overriding consideration, and because Christy's calculations do show that M_v(RR) is a function of $\langle P\rangle_{ab}$, we prefer to view Table 13 only as a general check of $\langle M_v(\text{RR})\rangle$ determined by other means (Woolley *et al.* 1965; van Herk 1965; Christy 1966), and to take the detailed value for each cluster from Christy's (1966) theory, as in the next section.

b) *Distances from Independent Values for M_v(RR)*

From the observed shortest period of the Bailey type *ab* RR Lyrae stars in the various clusters, Christy (1966) calculates $L_{bol}(\text{RR}) = 1.44 \times 10^{35}$ ergs sec^{-1} for M3 and 1.78×10^{35} ergs sec^{-1} for M15. These can be changed to M_{bol} by adopting values of L_{bol} and M_{bol} for the Sun. The value of $(L_{bol})_\odot$ is probably known to about 1 percent, and was adopted by Christy to be 3.90×10^{33} ergs sec^{-1} following Allen (1963). However, $(M_{bol})_\odot$ depends on the (arbitrary) choice of the zero point for the bolometric correction

(adopted as −0.07 after Popper [1959]), and on the apparent V-magnitude of the Sun, which is not known to within better than 0.1 mag. Christy takes the value $V = -26.78$, adopted by Allen (1963). This is a mean of $V = -26.73$ measured by Stebbins and Kron (1957), and $V = -26.80$ from a discussion of all modern data by Martinov (1959).

Adopting $L_\odot = 3.90 \times 10^{33}$ ergs sec^{-1}, $(M_v)_\odot = 4.79$, $(M_{bol})_\odot = +4.72$, and B.C.(RR) = 0.00 (Morton and Adams 1968), Christy's calculated L(RR) transform to $M_v(\mathrm{RR})_{M3} = 0.80$, and $M_v(\mathrm{RR})_{M15} = 0.57$. Dickens (1971) lists $M_v(\mathrm{RR})_{M92} = 0.46$ on the same system, using Christy's precepts. Note that if Stebbins and Kron's value of $V(_\odot) = -26.73$ had been adopted, then $(M_V)_\odot = 4.84$ rather than 4.79, and the M_v(RR) values would be 0.05 mag fainter. This affects the cluster distances, but not the crucial quantity $L/L_\odot$. However, because it is conventional to do so and because it is convenient, we shall express the cluster parameters in terms of M_v. Consistent adoption of $(M_{bol})_\odot =$

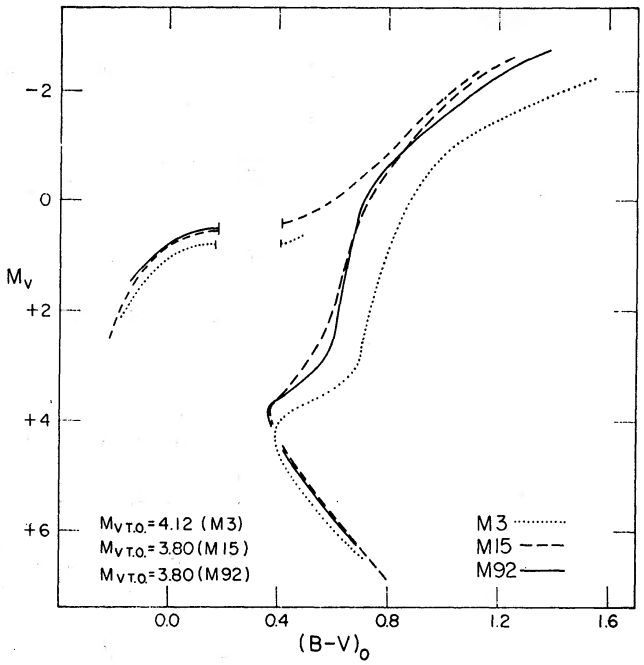

FIG. 17.—Adopted normalization of M3, M15, and M92 by using Christy's values of M_v for RR Lyrae stars in each cluster. Corrections for reddening only have been applied to $B - V$. The well-known dependence of M_v for red giants on metal abundance is evident.

4.72 and Popper's (1959) zero point to the bolometric correction leads to correct results whose only uncertainties are (1) Christy's theory for L_{bol}(RR), (2) $(L_{bol})_\odot$, and (3) the variation of the bolometric correction with T_e.

The mean apparent magnitude for the RR Lyrae stars in each cluster is given in column (7) of Table 13. These, combined with Christy's calculated M_v, lead to distance moduli of $(m - M)_0 = 14.83$ for M3, $(m - M)_0 = 14.93$ for M15, and $(m - M)_{AV} =$ 14.63 for M92. The C-M diagrams of Figures 4, 11, and 13 can now be transformed to M_V, $(B - V)_0$ corrected for reddening, with the result shown in Figure 17. Note that the vertical positioning in Figure 17 is obtained independently of data on main-sequence colors, blanketing corrections, $\delta(U - B)$ values, and $E(B - V)$. This is the great power of method *b*.

M13 cannot be placed in Figure 17 by this method because there are too few RR Lyrae stars to apply Christy's equation.

V. THE CURIOUS CASE OF M13

The few RR Lyrae stars in M13 are unusual. Sawyer (1955) lists ten variables, six of which have $P > 1^d$. Of the remaining four, periods are available for Nos. 5, 8, and 9, and amplitudes are listed by Sawyer. The periods ($0^d.381793$ for No. 5; $0^d.750318$ for No. 8; $0^d.392713$ for No. 9) from Sawyer (1955) and Osborn (1969*a*, *b*) are abnormally long compared with variables in the general field (Preston 1959, Figs. 6 and 8) and in other clusters except for ω Cen (Baade and Swope 1961, Fig. 26; Dickens and Saunders 1965). Furthermore, the amplitude of No. 8 ($A_B = 1.4$ mag according to Sawyer [1955]; 0.90 by Arp [1955]; 1.14 by Osborn [1969*a*]) is considerably larger than for any variable in M3, M15, or ω Cen at its period. These facts suggest that the variables in M13 are brighter than those in M15, M92, and ω Cen.

The modulus of M13 has been estimated in two ways.

1. Variable 8, with $P = 0^d.75$, $A_B = 1.15$, has been plotted in the period-amplitude diagram for variables in ω Cen (Dickens and Saunders 1965, Fig. 3), M15 (Sandage *et al.* 1971), and M3 (Roberts and Sandage 1955, Fig. 5). The star deviates from the mean relations by $\Delta \log P = 0.082$ for ω Cen, 0.075 for M15, and 0.130 for M3. There is every reason to believe that the period-amplitude relations in given clusters differ from one another by the period ratio given by the Oosterhoff-Sawyer phenomenon, and therefore that the $\Delta \log P$ are related to M_v(RR) by the theory which explains the phenomenon. Christy's (1966, p. 170) equation $P \propto (L/L_\odot)^{0.6}$ predicts $\Delta M_v = 4.16\, \Delta \log P$. Hence, we obtain for Var 8 in M13, $\Delta M_v = 0.34$ mag relative to ω Cen (No. 8 is brighter), 0.31 mag brighter than variables in M15, and 0.54 mag brighter than M3. Adopting as before $M_v = 0.57$ for ω Cen and M15, and 0.80 for M3 (Christy 1966, Table 4) gives M_v(M13, No. 8) = 0.23, 0.26, and 0.26 for the three calibrating clusters, respectively, with a mean of M_v(M13, No. 8) = 0.25.

2. Comparing the C-M diagram of M13 with those in Figure 17, and requiring the M13 main sequence to be intrinsically redder than those in M15 and M92 by $\Delta(B - V) = 0.03$ mag due to increased blanketing (see Table 4 of Wildey *et al.* [1962] using the $\langle \delta \rangle$ values in the second part of Table 13) gives $(m - M)_{AV} = 14.70$. From V(RR) = 14.57, the absolute magnitude becomes M_v(M13, No. 8) = -0.13. The method is not as fundamental as method *a* in § IV because it assumes that the main sequences of M13 and M15 coincide in the (M_v, log T_e)-plane despite the difference in Z.

The mean of all values from methods (1) and (2) give M_v(M13, No. 8) = 0.15, or $(m - M)_{AV} = 14.42$ with an uncertainty of at least 0.2 mag. We adopt this value in the subsequent discussion.

The resulting composite C-M diagram is shown in Figure 18, which is Figure 17 with M13 added. The RR Lyrae stars in M13 are anomalously bright by $\sim$0.65 mag relative to those in M3, and in fact are brighter than the blue end of their own cluster's horizontal branch.

The effect is further shown by ΔM_v between the variables and the main-sequence turnoff. For M3, this difference is ΔM(TO $-$ RR) = 3.32 mag while it is 3.95 mag for M13 despite the fact that Δ mag = 3.35 in M13 between the turnoff and the horizontal branch. These features are the basis for believing that variables in M13 may be connected with the evolution of the asymptotic branch rather than the horizontal branch (§ IV).

VI. AGES

a) Input Data

According to the two most recent sets of theoretical models (Iben and Rood 1970; Demarque, Mengel, and Aizenman 1971), ages are a sensitive function of M_{TO}, Y, and Z. Figure 18 gives M_v(TO). Christy's theory (1966) gives Y for those clusters where the color of the blue edge of the RR Lyrae strip is known. Spectroscopic studies give Z.

i) $L_{bol}(TO)$

The main-sequence turnoff is defined as the luminosity where $B - V$ is bluest in each cluster. The M_v(TO) of Figure 18 are converted to $L_{bol}/L_\odot$ in three steps. (*a*) Line deblanketing has made V(observed) too faint for globular-cluster stars relative to Hyades-like stars of the same T_e due to the combination of blocking and back warming. The corrections are taken from Table 4 of Wildey *et al.* (1962), with data in Table 10 used for each cluster. They average −0.07 mag for all four clusters. (*b*) Stars at the turnoff have $(B - V)_{0,c} \simeq 0.60$ after applying blanketing corrections to the colors. The bolometric correction is then −0.07 (Morton and Adams 1968, Table 2), and is the same for all clusters. (*c*) Applying both corrections to M_v(TO), as read from Figure 18, gives M_{bol}(TO), which is combined with $(M_{bol})_\odot = 4.72$ (see § IV*b*) to give log $L/L_\odot$. The results are log $L_{bol}/L_\odot = 0.292$, 0.424, and 0.424 for M3, M15, and M92, respectively. For M13, log $L/L_\odot = 0.312$ with more uncertainty.

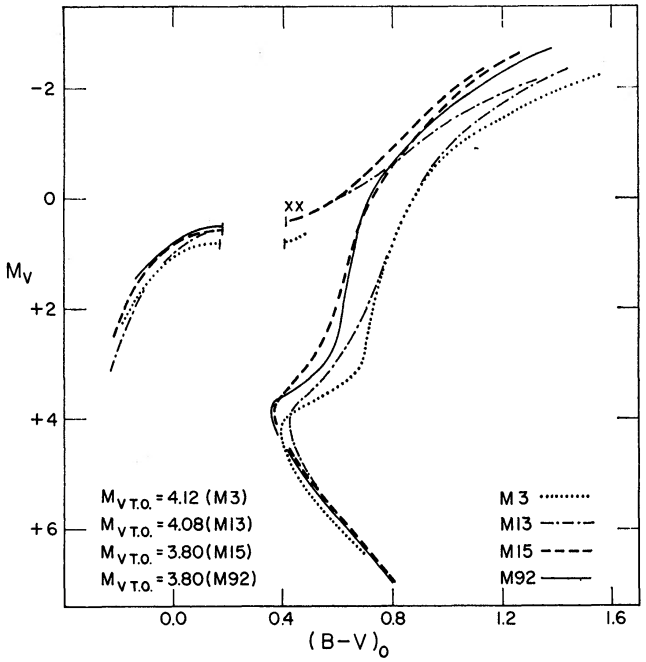

FIG. 18.—Same as Fig. 17 but with M13 added, using the method in the text for normalization. Two RR Lyrae stars in M13, with Arp's values used, are plotted as crosses. The turnoff luminosities are listed.

ii) *Helium Abundance*

Interpolation in Christy's (1966) Table 1, if $(M_{bol})_\odot = 4.72$ is adopted, gives

$$Y = 1.600(B - V)_{BE}{}^{0,c} - 0.34\,\mathfrak{M}/\mathfrak{M}_\odot - 0.16\,M_v + 0.901\,, \qquad (1)$$

which differs slightly from that given elsewhere (Sandage 1969*a*) due to a different value of $(M_{bol})_\odot$. Here, $(B - V)_{BE}{}^{0,c}$ is the color at the blue edge of the RR Lyrae strip corrected for reddening and blanketing to the SU Dra abundance system ($\Delta S = 6$), and $\mathfrak{M}/\mathfrak{M}_\odot$ and M_v are respectively the mass and absolute magnitude of stars at this edge. The adopted parameters are shown in Table 14, taken from § IV*b*, Figure 18, and the previous study (Sandage 1969*a*). Equation (1) then gives the tabulated values of Y. The values for M13 refer to the beginning of the blue edge of the horizontal branch from Figures 6 and 18 and may therefore not accurately define the edge of the instability strip, with a resulting uncertainty in Y.

iii) *Metal Abundance*

Spectrographic abundances have been determined for giant stars in M92 and M13 by Helfer, Wallerstein, and Greenstein (1959), and later modified by Wallerstein and Helfer (1966) to account for Rayleigh scattering in M92. It is not certain that these atmospheric Z values for giants are the same as the interior values for main-sequence dwarfs, but because this is the only nonspeculative way to proceed at the moment, we shall assume they are identical.

Wallerstein and Helfer adopt $[\mathrm{Fe/H}] \equiv \log(\mathrm{Fe/H})_{\mathrm{CL}} - \log(\mathrm{Fe/H})_{\odot} = -2.1$ for M92, and -1.4 for M13. From the evidence of Morgan, Deutsch, and § III*c* of this paper, it seems likely that [Fe/H] is the same for M15 and M92. The case of M3 is more difficult. Table 10 suggests that $[\mathrm{Fe/H}]_{\mathrm{M3}} > [\mathrm{Fe/H}]_{\mathrm{M13}}$, while the ultraviolet excess of the giants (§ III*c*) and the Morgan-Deutsch data require the opposite. In the age-dating calculations we carry two values of $[\mathrm{Fe/H}]_{\mathrm{M3}}$ of -1.2 and -1.6, but suggest that the lower metal abundance is more probable. The [Fe/H] values are changed to Z by adopting $Z_{\odot} = 0.020$ (e.g., the summary by Morton 1968), and are listed in Table 14.

TABLE 14

INPUT PARAMETERS AND RESULTS FOR Y AND Z

Cluster	$(B-V)_{\mathrm{BE}}{}^{0,c}$	M_v(BE)	$\mathfrak{M}/\mathfrak{M}_{\odot}$	Y	[Fe/H]*	log Z†
M3.....	0.175	0.80	0.55	0.306	(−1.6)(−1.2)	(−3.3)(−2.9)
M13.....	(0.170)	(0.53)	0.55	(0.357)	−1.4	−3.1
M15.....	0.170	0.57	0.55	0.351	−2.1	−3.8
M92.....	0.195	0.46	0.55	0.328	−2.1	−3.8

* $[\mathrm{Fe/H}] \equiv \log(\mathrm{Fe/H})_{\mathrm{CL}} - \log(\mathrm{Fe/H})_{\odot}$.

† From penultimate column with the value $Z_{\odot} = 0.02$ used.

b) Ages Calculated from Iben and Rood's Models

Iben and Rood (1970, hereafter called IR) have computed isochrones from their detailed tracks, and give an interpolation equation for ages as

$$\log T_9 = \frac{\log L_{\mathrm{TO}}/L_{\odot} + (0.92 + 0.11 \log Z)Y + 0.219 \log Z - 0.789}{0.10 \log Z - 0.59} \qquad (2)$$

in the range $0 < Y \lesssim 0.3$, $10^{-3} > Z > 10^{-5}$. For equal L_{TO} and Y, clusters with *lower* Z are *older*, as first pointed out by Simoda and Iben (1968), and more recently confirmed by Demarque *et al.* (1970). The consequence is that if clusters of different Z are the same age (and have the same helium abundance), those of lower Z must have a brighter turnoff. Interestingly enough, *this is the same sense as Figure 18*, where the M3 and M13 turnoff points are significantly fainter than those in M15 and M92.

Application of equation (2) to each cluster, by the use of input data just discussed, gives ages listed in Table 15 under T(IR). The clustering of T near 11.5×10^9 years is evident, but it should be remembered that log Z for M3 is most probably lower than that of M13, making $(13.8 \times 10^9)_{\mathrm{M3}}$ years the more probable value. Because of the suspicion that the M3 photometry still contains systematic errors (§ IV*a*[iv]), we consider the observational problem still open, pending new M3 photometry.

c) Ages Calculated from Models of Demarque et al.

An important independent study of turnoff luminosities as a function of age, Y, and Z has been made by Demarque *et al.* (1970, hereafter called DMA). The functional dependences of Iben and Rood are generally confirmed, but the ages are *smaller* for

given log $L_{TO}/L_{\odot}$, Y, and Z. Interpolating in Figure 8 of DMA and comparing with equation (2) gives $T(\mathrm{IR})/T(\mathrm{DMA}) \simeq 1.2$ in the relevant range of parameters near $M_{bol} = +4.0$, $Y = 0.25$, and $\log Z = -3.0$. Adopting this ratio gives DMA ages listed in column (8) of Table 15. From the present data there is no real evidence for a variation of helium abundance among the four clusters. Columns (9) and (10) give ages from each of the two sets of models if the helium abundance is taken to be constant at $Y = 0.328$, which is the mean from M3, M15, and M92.

d) Ages of Other Clusters

The only other clusters with main-sequence data are 47 Tuc (Tifft 1963), M2 and M5 (Arp 1959, 1962), and NGC 6397 (Eggen 1960). All four have termination points near $M_v \simeq +4.0$ and conform in a general way to Figure 18. The helium abundance in 47 Tuc is unknown and cannot be found by Christy's method because of the nature of its horizontal branch. Arp's data for M2 and M5 show $(B - V)_{BE}{}^0 \simeq 0.2$, which again indicates $Y \simeq 0.3$. From this it is clear that the ages are not grossly different from those in Table 15. However, to calculate them on the present system depends on reconciling conflicting data for Z. For example, M5 is a Deutsch class A, whereas the Morgan class

TABLE 15

SUMMARY OF INPUT DATA AND AGES

Cluster (1)	M_v(TO) (2)	M_{bol}(TO) (3)	log $L/L_{\odot}$ (4)	Y (5)	log Z (6)	T_9(IR)* (7)	T_9(DMA)* (8)	T_9(IR)† (9)	T_9(DMA)† (10)
M3.....	4.12	3.99	0.292	0.306	−3.3‡	13.8	11.5	13.4	11.2
M3.....	4.12	3.99	0.292	0.306	−2.9‡	11.9	9.9	11.6	9.6
M13....	(4.08)	(3.94)	(0.312)	(0.357)	−3.1	(11.3)	(9.4)	(11.8)	(9.8)
M15....	3.80	3.66	0.424	0.351	−3.8	11.3	9.4	11.6	9.6
M92....	3.80	3.66	0.424	0.328	−3.8	11.6	9.7	11.6	9.6

* The rms error is of order $\epsilon T/T \simeq 0.28$.

† Ages if constant $Y = 0.328$ is adopted for all clusters.

‡ Log $Z = -3.3$ is the more likely value for M3.

is II rather than III or IV. The mean period of the RR Lyrae type *ab* is about the same as M3 ($\langle P \rangle = 0^d.55$), but the ultraviolet excess measured by Eggen (1969, Fig. 8) is considerably larger than for M3, although earlier data by Arp (1962) lead to the opposite conclusion.

Nevertheless, the fact that all eight clusters have remarkably similar turnoff luminosities ($M_v \simeq +4.0$), and that the range of Z is close to that of Table 15 (47 Tuc has higher metal abundance such that log $Z \simeq -2.7$) means that the ages of all eight must be closely the same. We consider this to be the most important result of the present investigation.

The errors, discussed next, are large enough that the ages in Table 15 could be identical to within the limits required on the collapse picture of the Galaxy discussed by Eggen, Lynden-Bell, and Sandage (1962, hereafter called ELS).

e) Errors

Aside from the 20 percent difference between the two sets of models, the ages in Table 15 are uncertain due to observational errors. Uncertainties in the turnoff luminosities are of the order $\Delta M_{bol} \simeq \pm 0.2$ mag due to errors in the distance modulus and to the vagueness of reading the C-M diagram at its bluest main-sequence color. Errors in Y are about ± 0.10 due to errors in the input data required in equation (1), coupled with possible uncertainties in the temperature scale for RR Lyrae stars (e.g., Strom 1969). Uncertainties in Z can easily be a factor of 3 either way, or $\Delta \log Z = \pm 0.48$.

With these errors, equation (2) with $\langle \log L_{TO}/L_{\odot} \rangle = 0.35$, $\langle \log Z \rangle = -3.5$, and $\langle Y \rangle = 0.30$, gives

$$[\partial T/T]_{Z,Y} = 1.06\Delta L/L \simeq \pm 0.21\,, \quad [\partial T/T]_{Z,L} = 0.57\Delta Y \simeq \pm 0.06\,,$$
$$[\partial T/T]_{L,Y} = 0.4\Delta \log Z \simeq \pm 0.19\,. \tag{3}$$

The dependence on L and Z is particularly strong, as emphasized by Simoda and Iben (1968), Iben and Rood (1970), and Demarque *et al.* (1970).

Combining these errors by the sum of the squares gives an rms error of $\epsilon T/T \simeq \pm 0.28$, which is about 3×10^9 years for all clusters in Table 15. This error is large and unfortunately cannot be appreciably reduced by foreseeable improvements in the data. To test the ELS collapse picture requires a method which is more accurate differentially (see § VII).

f) Other Age Determinations

We have not used age-dating methods which use the temperature of the main-sequence turnoff, because the calculated model radii are extraordinarily sensitive to the assumed convective mixing length (e.g., Demarque 1968). On the contrary, Figure 10 of Demarque shows that $\log L_{TO}/L_{\odot}$ is largely *independent* of l/H, and therefore that luminosities provide a reliable age parameter whereas surface temperature does not.

Many discussions of ages have appeared in the literature prior to the IR and DMA models. The most complete were by Demarque (1967*a*), Iben and Faulkner (1968), and Simoda and Iben (1968), where the essential functional dependence of age on Y and L were displayed. However, in these models, ages for given L, Y, and Z values were considerably longer than those of the latest DMA and IR models adopted here. Furthermore, the low ages of 9×10^9 years favored by Iben and Faulkner (1968) from their global-consistency arguments were inconsistent with *observational* results on M_{bol} (TO and M_{bol} (RR) known already in 1968.

For example, Iben and Faulkner calculated that if $T = 9 \times 10^9$ years for $Y = 0.33$ and $Z = 2 \times 10^{-4}$, then $M_{bol}(RR) = -0.26$, and $M_{bol}(TO) = +3.35$. These model magnitudes are 0.6 mag brighter than the observed values. Iben and Faulkner's conclusions, then, should have been that $T = 17 \times 10^9$ years if a fit to both the data and their models (see Table 3 of Iben and Faulkner 1968 for $Y = 0.35$) had been made.

Because of these earlier difficulties, it is very encouraging that the present independent models of IR and DMA both agree in giving $T \simeq 10 \times 10^9$ years if the observational data are used directly. It is equally encouraging that the ages are shorter than the Hubble time, currently estimated to have a lower limit of $H_0^{-1} = 13 \times 10^9$ years [i.e. H_0 (upper) = 75 km sec^{-1} Mpc^{-1}]. It now seems probable that H_0 may in fact be closer to 50 km sec^{-1} Mpc^{-1} (i.e., $H_0^{-1} = 19 \times 10^9$ years) than to 75 (Sandage 1968), and this gives some margin for appreciable deceleration of the expansion of the Universe (such as $q_0 = +1$) and still is consistent with the simple Friedmann models of the Universe with the low ages in Table 15.

VII. ARE ALL HALO CLUSTER AGES EQUAL? THE OOSTERHOFF-SAWYER EFFECT

In the ELS model for the formation of the Galaxy, the first-generation stars were formed during a fast collapse when the gravitational potential was changing on a time scale short compared with the galactic-rotation period. The collapse must have been fast, because if it had not been, the plunging orbits observed for the Population II stars could not have been produced due to the adiabatic invariance of the orbital eccentricity. Because $T_{rot} \simeq$ a few times 10^8 years, the globular clusters in the halo are expected to be of equal age to within this spread, if the ELS picture is correct.[1]

[1] This point of view differs from that given by Rood and Iben (1968) because they maintain that a *slow* collapse (i.e., $T_{collapse} > T_{rot}$) is possible in which plunging orbits will still be produced if the gaseous primeval Galaxy is pressure-supported and is in equilibrium. The pressure support is relieved on indi-

Although the *absolute* ages of Table 15 have intrinsic errors of $\epsilon T/T \simeq 0.3$ due to zero-point uncertainties in L(TO) and log Z, relative ages can be determined more accurately by several methods. One such determination (Sandage 1969*a*), which uses color *differences* of the turnoff, is suspect because of the Simoda-Iben (1968) effect. However, another more powerful method seems to exist which not only gives $\Delta T/T$ between the clusters but also explains the long-known but mysterious correlation between the metal abundance and the Oosterhoff-Sawyer mean period difference between clusters. The clue, already present in the close agreement of the listed ages in Table 15, is further developed here by recalling the following facts.

1. Clusters can be divided into two Oosterhoff-Sawyer groups such that the mean period of Bailey type *ab* stars is about $\langle P \rangle_{ab} \simeq 0^d.55$ in group I, and $0^d.65$ in group II.

2. Clusters in group II have lower metal abundance than in group I. For example, M15 and M92 are in group II whereas M3 is in group I. This correlation, first suggested by Arp (1955), is now very well established.

3. The explanation for point 1 appears to be that the horizontal branch for group II clusters is brighter than for group I (Sandage 1958; Christy 1966) by about 0.3 mag. (This fact has already been used in § IV*b* which itself leads to the ages in Table 15.)

4. A new fact emerges from the present data by comparing the C-M diagrams of Figures 4, 6, 11, and 13. The magnitude difference between the turnoff point and the horizontal branch is the same for all clusters ($\Delta M_v = 3.35$ to within the observed accuracy of ± 0.1 mag), despite the difference in metal abundance. This means that as the absolute magnitude at turnoff moves up or down for one cluster relative to another, the horizontal branch will change by the same amount.

These points can be combined in the following way. The Simoda-Iben effect shows that, for the same Y, clusters of lower Z must have brighter turnoff luminosities if they are the same age. The dating equation (2) predicts that

$$\Delta \ln T_9 \simeq 1.06\, \Delta \ln L_{\rm TO} + \frac{0.265}{\log_{10} e}\, \Delta \log Z \tag{4}$$

near $Y = 0.3$ and $\log Z = -3.5$, which means that

$$\Delta T/T \simeq 1.06\, \Delta \mathrm{mag(TO)} + 0.611\, \Delta \log Z\,, \tag{5}$$

where Δmag is the difference in the magnitude at main-sequence turnoff for a given metal-abundance difference $\Delta \log Z$.

For equal age, the magnitude at the *main sequence* must then be related to the metal abundance by

$$\Delta m \simeq -0.58\, \Delta \log Z \tag{6}$$

in the sense that clusters with lower metal abundance have brighter turnoff magnitudes.

Now remarkably the *main-sequence condition of equation (6) is the same as the generalized Oosterhoff-Sawyer elect as noted in a different context in § IV for the horizontal branch.*

---

vidual stars when they form from the gas due to the reduced surface area of the stellar disk, and the stars plunge toward the center. This model was considered and rejected by ELS because "if the gas was hot enough to support itself against the self-gravity of the entire galaxy, it was certainly hot enough to support itself against the gravity of any density fluctuation of protostellar size." The collapse free-fall time was also questioned. In calculating this time, Rood and Iben use parameters which do not apply to our Galaxy. The free-fall equation is $T_{\rm collapse} \simeq 0.6 \times 10^9\, (D/50\ \mathrm{kpc})^{3/2} (10^{11}\, \mathfrak{M}_\odot/\mathfrak{M}_{\rm eff})^{1/2}$ years, where D is the distance from the center where stars are formed, and $\mathfrak{M}_{\rm eff}$ is the galactic mass interior to this distance. Most of the stars discussed by ELS have $D \leq 25$ kpc. The effective mass of the galaxy at this distance will be the mass now within a distance from the center of the present equilibrium galaxy where the angular momentum is that of these Population II stars (i.e., $R \simeq 5$ kpc). This is of order $10^{11}\, \mathfrak{M}_\odot$; hence $T_{\rm collapse} \simeq$ a few $\times 10^8$ years as required by ELS, rather than the larger numbers used by Rood and Iben. I am indebted to Donald Lynden-Bell for discussion on these points (see also Lynden-Bell 1967).

Between Oosterhoff-Sawyer groups I and II, the metal abundance differs by $\Delta\log Z \approx 0.5$ (Table 15). By point 3 above, the magnitude of the horizontal branch differs by $\Delta\text{mag} \simeq 4.16\,\Delta\log P = 0.3$ mag. The ratio of Δmag to $\Delta\log Z$ via the Oosterhoff-Sawyer approach is then 0.60, *which is in the same sense and by the same amount as the main-sequence equation* (*6*).

What limits can be placed on $\Delta T/T$ by this method? The metal-abundance ratio may be uncertain by $\epsilon\Delta\log Z = \pm 0.2$ about a mean value of $\Delta\log Z = 0.50$. Hence, if we use $\Delta\text{mag} = 0.30$ between Oosterhoff-Sawyer groups, we obtain $\Delta m/\Delta\log Z = 0.60$ $(+0.40, -0.17)$, where all the error is assumed to be in log Z. The most probable value (0.60), when substituted in equation (5) along with $\Delta\text{mag} = 0.30$, gives

$$\Delta T/T = 0.014 \tag{7}$$

with limits of $\Delta T/T = 0.135$ and 0.108 using $\Delta\log Z = 0.50 \pm 0.2$.

Equation (7) is the final result when the best observational data available are used. The errors are unfortunately large, and the method cannot yet be used to test the ELS requirement at a high confidence level, although the most probable result given by equation (7) and Table 15 is $\Delta T \simeq 10^8$ years. But the most important aspect of the method would seem to be the explanation for the previously known correlation of Oosterhoff-Sawyer groups with metal abundance—a result which is now seen to be *required* if the clusters are of nearly equal age.

VIII. CONCLUSIONS

The remarkable similarity between the relative ages of globular clusters, together with their absolute value near 10×10^9 years, has well-known consequences for the history of the Galaxy and the Universe. Added to these results is the evidence for helium abundance near $Y = 0.3$ from Christy's calculations, from the present work, and from the studies of Hartwick (1970). This value is close to that required for pristine production in the primeval fireball.

The present data are consistent with big-bang Friedmann models ($\Lambda = 0$) as regards time scales, but only if the Hubble constant is less than 75 km sec^{-1} Mpc^{-1}, or if the deceleration parameter q_0 is less than $+1$. We are in some slight trouble when we use the currently adopted cosmological parameters of $H_0 = 75$ ($H_0^{-1} = 13 \times 10^9$ years, $q_0 = +1$), because the Friedmann time is then $T_F = 0.571\ H_0^{-1} = 7.4 \times 10^9$ years, which is much too short. Of the two numbers q_0 and H_0, H_0 is the more uncertain as regards the time scale, but a lower limit of $H_0 = 50$ km sec^{-1} Mpc^{-1} seems secure (Sandage 1968). Unless, then, q_0 can be reduced, an *upper* limit for the Friedmann time is $T_F = 0.57\ H_0^{-1} \times 10.9 \times 10^9$ years for $q_0 \simeq +1$, but with large errors of about a factor of 1.5 due to the large error in q_0.

I believe the most certain conclusion from the present work as regards cosmology is that the previously reported long time scales derived by the use of globular clusters (i.e., $T_e \gtrsim 15 \times 10^9$ years) are too large, and that the age of our Galaxy, counted from the time of rapid collapse, is closer to 10×10^9 years.

It is a particular pleasure to acknowledge the extensive and efficient help of the night assistants on Mount Wilson and Palomar during the past 13 years in the course of this project. Especially helpful were Eugene Hancock, Alfred Olmstead, and Henry Schaefer on Mount Wilson, and Robert Seares, Gary Tuton, and William van Hook on Palomar. As regards the analysis of the material, Basil Katem undertook most of the photographic smoothing-measurements with his usual skill, devotion, and meticulous attention to detail. It is a special pleasure to acknowledge his help. It is also a privilege to thank Felice Woodworth for her excellent preparation of the diagrams for publication.

APPENDIX

As an aid in numerically defining the C-M diagrams of Figures 4, 6, 11, and 13, representative points from these plots are listed in Table A1. The tabulated values have been read from the large-scale original plots, and no corrections have been applied for reddening or absorption for M3, M13, and M92. Corrections of $E(B - V) = 0.12$, $A_v = 0.36$ mag, have been applied to the original data of M15.

TABLE A1

MEAN POINTS READ FROM THE C-M DIAGRAMS

M3				M13				M15				M92			
V	B-V	V	B-V	V	B-V	V	B-V	V_0	$(B-V)_0$	V_0	$(B-V)_0$	V	B-V	V	B-V
Giants		19.50	0.41	Giants		19.85	0.55	Giants		20.94	0.65	Giants		19.95	0.55
12.62	1.55	20.00	0.47	12.05	1.62	20.20	0.60	12.44	1.20	21.23	0.70	11.90	1.40	20.25	0.60
12.70	1.50	20.50	0.54	12.05	1.50	20.50	0.65	12.75	1.10	21.54	0.75	12.09	1.30	20.55	0.65
12.90	1.40	21.00	0.64	12.16	1.40	21.02	0.75	13.20	1.00	Asymptotic		12.39	1.20	20.80	0.70
13.14	1.30	21.25	0.70	12.40	1.30	21.27	0.80	13.72	0.90	12.62	1.10	12.75	1.10	21.10	0.75
13.40	1.20	Asymptotic		12.70	1.20	21.50	0.85	14.35	0.80	13.00	1.00	13.15	1.00	21.36	0.80
13.66	1.10	13.40	1.15	13.09	1.10	21.70	0.90	14.70	0.75	13.50	0.90	13.58	0.90	21.63	0.85
14.04	1.00	13.54	1.10	13.55	1.00	Asymptotic		15.22	0.70	14.00	0.80	14.11	0.80	Asymptotic	
14.25	0.95	13.85	1.00	13.85	0.95	12.35	1.30	Subgiants		14.50	0.70	14.45	0.75	12.30	1.20
14.65	0.90	14.25	0.90	14.15	0.90	12.55	1.20	16.00	0.65	14.92	0.60	15.05	0.70	12.60	1.10
15.00	0.86	14.42	0.85	14.64	0.85	12.80	1.10	16.50	0.62	15.10	0.55	Subgiants		12.96	1.00
15.50	0.82	14.75	0.77	Subgiants		13.10	1.00	17.00	0.59	15.20	0.50	15.50	0.68	13.36	0.90
Subgiants		14.80	0.64	15.00	0.82	13.45	0.90	17.50	0.55	15.30	0.45	16.00	0.66	13.80	0.80
16.00	0.79	H Branch		15.50	0.79	13.85	0.80	17.88	0.50	H Branch		16.50	0.64	14.20	0.70
16.50	0.75	15.60	0.45	16.00	0.75	14.16	0.70	18.25	0.44	15.50	0.15	17.00	0.62	14.49	0.60
17.00	0.73	15.63	0.40	16.50	0.70	14.25	0.65	Main Seq.		15.52	0.10	17.40	0.60	14.76	0.50
17.50	0.70	15.63	0.17	17.00	0.65	H Branch		18.52	0.40	15.61	0.05	17.50	0.59	H Branch	
17.75	0.69	15.70	0.10	17.50	0.59	14.95	0.16	18.75	0.37	15.75	0.00	17.75	0.54	15.10	0.20
18.00	0.67	15.78	0.05	17.75	0.55	15.10	0.10	19.18	0.40	15.95	-0.05	17.90	0.50	15.15	0.15
18.25	0.61	15.95	0.00	18.00	0.48	15.15	0.05	19.60	0.45	16.25	-0.10	18.10	0.45	15.28	0.10
18.50	0.52	16.15	-0.05	18.15	0.45	15.46	0.00	20.00	0.50	16.62	-0.15	18.26	0.40	15.35	0.05
18.75	0.43	16.44	-0.10	Main Seq.		15.71	-0.05	20.30	0.55	17.23	-0.20	Main Seq.		15.55	0.00
Main Seq.		16.80	-0.15	18.50	0.42	16.05	-0.10	20.63	0.60			18.40	0.38	15.75	-0.05
19.00	0.40	17.00	-0.17	18.75	0.43	16.50	-0.15					18.70	0.40	16.00	-0.12
19.25	0.40			19.00	0.45	17.20	-0.20					19.18	0.45	16.11	-0.12
				19.45	0.50	17.50	-0.22					19.60	0.50		

REFERENCES

Allen, C. W. 1963, *Astrophysical Quantities* (2d ed.; London: Athlone Press), **2**, 161.
Arp, H. C. 1955, *A.J.*, **60**, 317.
———. 1959, *ibid.*, **64**, 441.
———. 1962, *Ap. J.*, **135**, 311.
———. 1964, in *Stars and Stellar Systems*, Vol. **5**, ed. A. Blaauw and M. Schmidt (Chicago: University of Chicago Press), chap. 19.
Arp, H. C., Baum, W. A., and Sandage, A. R. 1953, *A.J.*, **58**, 4.
Arp, H. C., and Johnson, H. L. 1955, *Ap. J.*, **122**, 171.
Baade, W., and Swope, H. H. 1961, *A.J.*, **66**, 300.
Baum, W. A. 1952, *A.J.*, **57**, 222.
———. 1954, *ibid.*, **59**, 422.
Baum, W. A., Hiltner, W. A., Johnson, H. L., and Sandage, A. R. 1959, *Ap. J.*, **130**, 749.
Belserene, E. P. 1959, *A.J.*, **64**, 58.
Brown, A. 1951, *Ap. J.*, **113**, 344.
———. 1955, *ibid.*, **122**, 146.
Cayrel, R. 1968, *Ap. J.*, **151**, 997.
Christy, R. F. 1966, *Ap. J.*, **144**, 108.
———. 1968, *Quart. J.R.A.S.*, **9**, 13.
——— 1969, *J R A S. Canada*, **63**, 299
———. 1970, *ibid* , **64**, 8
Cousins, A. W. J., Eggen, O. J., and Stoy, R. H. 1961, *R.O.B.*, No. 25, p. E39.
Cousins, A. W. J., and Stoy, R. H. 1963, *R.O.B.*, No. 64, p. E103.
Crawford, D. L., and Barnes, J. V. 1969, *A.J.*, **74**, 1008.
Demarque, P. 1967*a*, *Ap. J.*, **149**, 117.
———. 1967*b*, *ibid.*, **150**, 943.
———. 1968, *A.J.*, **73**, 669.
Demarque, P., Mengel, J. G., and Aizenman, M. 1971, *Ap. J.* (preprint).

Dickens, R. J. 1971, *Ap. J.* (in press).
Dickens, R. J. and Saunders, J. 1965, *R.O.B.*, **101**, p. 101.
Eggen, O. J. 1959, *M.N.A.S., South Africa*, **18**, 91.
———. 1960, *ibid.*, **19**, 115.
———. 1965, *Ann. Rev. Astr. and Ap.*, **3**, 235.
———. 1968, *Ap. J.*, **153**, 195.
———. 1969, *ibid.*, **158**, 225.
Eggen, O. J., Lynden-Bell, D., and Sandage, A. 1962, *Ap. J.*, **136**, 748.
Eggen, O. J., and Sandage, A. R., 1962, *Ap. J.*, **136**, 735.
———. 1964, *ibid.*, **140**, 130.
Geyer, E. H. 1967, *Zs. f. Ap.*, **66**, 16.
Hartwick, F. D. A 1970, *Ap. J.*, **161**, 845.
Helfer, H. L., Wallerstein, G., and Greenstein, J. L. 1959, *Ap. J.*, **129**, 700.
Herk, G. van. 1965, *B.A.N.*, **18**, 71.
Iben, I., and Faulkner, J. 1968, *Ap. J.*, **153**, 101.
Iben, I., and Rood, R. T. 1970, *Ap. J.*, **159**, 605.
Jenkins, L. F. 1952, *General Catalog of Trigonometric Parallaxes* (New Haven, Conn.: Yale University Observatory).
Johnson, H. L., and Morgan, W. W. 1953, *Ap. J.*, **117**, 313.
Johnson, H. L., and Sandage, A. R. 1956, *Ap. J.*, **124**, 379.
Kadla, Z. I. 1968, *Astr. Zh.*, **45**, 541.
Kinman, T. D. 1959, *M.N.R.A.S.*, **119**, 538.
Lynden-Bell, D 1967, *in I A.U Symposium 31*, ed. H van Woerden (London: Academic Press), Paper 44, p 257.
Martinov, D. Yu. 1959, *Soviet Astr.—A.J.*, **3**, 633.
McClure, R. D., and Racine, R. 1969, *A.J.*, **74**, 1000.
McNamara, D. H., and Langford, W. R. 1969, *Pub. A.S.P.*, **81**, 141.
Melbourne, W. G. 1960, *Ap. J.*, **132**, 101.
Mihalas, D. 1966, *Ap. J. Suppl.*, **13**, 1.
Morgan, W. W. 1959, *A.J.*, **64**, 432.
Morton, D. C. 1968, *Ap. J.*, **151**, 285.
Morton, D. C., and Adams, T. F. 1968, *Ap. J.*, **151**, 611.
Newell, E. B. 1970, *Ap. J.*, **159**, 443.
Newell, E. B., Rodgers, A. W., and Searle, L. 1969*a*, *Ap. J.*, **156**, 597.
———. 1969*b*, *ibid.*, **158**, 699.
Osborn, W. 1969*a*, *A.J.*, **74**, 108.
———. 1969*b*, *I.A.U. Inf. Bull. Var. Stars*, Konkoly Obs. No. 350.
Popper, D. M. 1959, *Ap. J.*, **129**, 647.
Preston, G. 1959, *Ap. J.*, **130**, 507.
Roberts, M. S., and Sandage, A. 1955, *A.J.*, **60**, 185.
Rood, R., and Iben, I. 1968, *Ap. J.*, **154**, 215.
Sandage, A. 1953, *A.J.*, **58**, 61.
———. 1958, *in Stellar Populations*, ed D. O'Connell (Amsterdam: North-Holland Publishing Co.), p. 41.
———. 1964, *Observatory*, **84**, 245.
———. 1968, *Ap. J.* (*Letters*), **152**, L149.
———. 1969*a*, *Ap. J.* **157**, 515.
———. 1969*b*, *ibid.*, **158**, 1115.
Sandage, A., and Eggen, O. J. 1959, *M.N.R.A.S.*, **119**, 278.
Sandage, A., and Katem, B. 1964, *Ap. J.*, **139**, 1088.
Sandage, A., Katem, B., and Kristian, J. 1968, *Ap. J.* (*Letters*), **153**, L129.
Sandage, A., Sandage, M., Katem, B., and Brueckel, F. 1971, in preparation.
Sandage, A., and Walker, M. F. 1955, *A.J.*, **60**, 230.
———. 1966, *Ap. J.*, **143**, 313.
Savedoff, M. P. 1956, *A.J.*, **61**, 254.
Sawyer, H. B. 1955, *Pub. David Dunlap Obs.*, Vol. **2**, No 2.
Simoda, M., and Iben, I. 1968, *Ap. J.*, **152**, 509.
Stebbins, J., and Kron, G. E. 1957, *Ap. J.*, **126**, 266.
Strom, S. E. 1969, *Ap. J.*, **156**, 177.
Tifft, W. G. 1963, *M.N.R.A.S.*, **126**, 209.
Wallerstein, G. 1967, *Pub. A.S.P.*, **79**, 317.
Wallerstein, G., and Helfer, H. L. 1966, *A.J.*, **71**, 350.
Wildey, R. L., Burbidge, E. M., Sandage, A., and Burbidge, G. R. 1962, *Ap. J.*, **135**, 94.
Woolley, R., Harding, G. A., Cassells, A. I., and Saunders, J. 1965, *R.O.B.*, No. 97, p. E3.